SANDIA REPORT
SAND2009-4743
Unlimited Release
Printed June 2009

Oxalate Co-precipitation Synthesis of Calcium Zirconate and Calcium Titanate Powders

Bernadette A. Hernandez-Sanchez, Bruce A. Tuttle, James A. Voigt, Diana L. Moore, Terry J. Garino, Patrick Mahoney, and Mark A. Rodriguez

Prepared by
Sandia National Laboratories
Albuquerque, New Mexico 87185 and Livermore, California 94550

Sandia is a multiprogram laboratory operated by Sandia Corporation,
a Lockheed Martin Company, for the United States Department of Energy's
National Nuclear Security Administration under Contract DE-AC04-94AL85000.

Issued by Sandia National Laboratories, operated for the United States Department of Energy by Sandia Corporation.

Available to DOE and DOE contractors from
U.S. Department of Energy
Office of Scientific and Technical Information
P.O. Box 62
Oak Ridge, TN 37831

Telephone: (865) 576-8401
Facsimile: (865) 576-5728
E-Mail: reports@adonis.osti.gov
Online ordering: http://www.osti.gov/bridge

Available to the public from
U.S. Department of Commerce
National Technical Information Service
5285 Port Royal Rd.
Springfield, VA 22161

Telephone: (800) 553-6847
Facsimile: (703) 605-6900
E-Mail: orders@ntis.fedworld.gov
Online order: http://www.ntis.gov/help/ordermethods.asp?loc=7-4-0#online

SAND2009-4743
Unlimited Release
Printed June 2009

Oxalate Co-precipitation Synthesis of Calcium Zirconate and Calcium Titanate Powders

Bernadette A. Hernandez-Sanchez
Ceramic Processing & Inorganic Materials
Sandia National Laboratories
P.O. Box 5800
Albuquerque, New Mexico 87185-MS1349

Bruce A. Tuttle
Electronic & Nanostructure Materials
Sandia National Laboratories
P.O. Box 5800
Albuquerque, New Mexico 87185-MS1411

Abstract

Fine powders of calcium zirconate ($CaZrO_3$, CZ) and calcium titanate ($CaTiO_3$, CT) were synthesized using a nonaqueous oxalate co-precipitation route from $Ca(NO_3)_2 \cdot 4H_2O$ and group(IV) *n*-butoxides ($Ti(OBu^n)_4$ or $Zr(OBu^n)_4$). Several reaction conditions and batch sizes (2–35 g) were explored to determine their influence on final particle size, morphology, and phase. Characterization of the as-prepared oxalate precursors, oven dried oxalate precursors (60–90 °C), and calcined powders (635–900 °C) were analyzed with TGA/DTA, XRD, TEM, and SEM. Densification and sintering studies on pressed CZ pellets at 1375 and 1400 °C were also performed. Through the developed oxalate co-precipitation route, densification temperatures for CZ were lowered by 125 °C from the 1500 °C firing temperature required for conventional mixed oxide powders. Low field electrical tests of the CZ pellets indicated excellent dielectric properties with dielectric constants of ~30 and a dissipation factor of 0.0004 were measured at 1 kHz.

ACKNOWLEDGMENTS

The authors thank Ms. B. McKenzie, Dr. L Brewer, and Ms. J. Wheeler for technical assistance and the office of Basic Energy Sciences of the Department of Energy for support of this work. Sandia is a multiprogram laboratory operated by Sandia Corporation, a Lockheed Martin Company, for the United States Department of Energy's National Nuclear Security Administration under contract DE-AC04-94AL85000.

CONTENTS

FIGURES

TABLES

NOMENCLATURE

ASD	Aerosol Spray Deposition
MLCC	Multilayer Ceramic Capacitors
CZ	$CaZrO_3$
CT	$CaTiO_3$
CZ Ox	$Ca\|Zr(O_2C_4)_3\|\cdot H_2O$
F	Fluorite Phase

1. INTRODUCTION

Large scale solution routes to perovskite ceramics, such as the alkaline earth zirconates (A^EZrO_3, A^E = Ca, Sr, Ba), titanates (A^ETiO_3, A^E= Ca, Sr), and their binary systems are of interest for their temperature insensitive dielectric properties. These perovskites have reasonable permittivities, very low dielectric loss, as well as extremely small positive (CZ, SZ) or negative (BZ, CT, ST) temperature coefficients which allow them to have minimal changes in their capacitance as a function of temperature.[1] Of this family, calcium zirconate titanate ($Ca(Zr_{1-x},Ti_x)O_3$) and its end members ($CaZrO_3$ (CZ) and $CaTiO_3$ (CT)) are well suited for our interests in pulse discharge capacitors and energy storage capacitors with minimal change in properties with temperature for DOE Defense Programs (DP) applications. Further, these dielectric materials could also impact DOE programs in microwave capacitors, electric hybrid and fuel cell vehicles. Central to all these applications, is the development of a synthetic solution route to highly active (particles with ultra fine (<1.0 μm) to nano (<0.1μm) sizes) calcium based perovskite powders that can be used to fabricate high quality thick films (> 20 μm) for multilayer ceramic capacitors (MLCC) through Aerosol Spray Deposition (ASD).

Improvement of MLCC film quality, by the synthesis of highly surface active ceramic powders, will facilitate low temperature densification and integration of ASD deposited thick films and tape cast layers. MLCCs use a parallel plate configuration where alternate layers of electrodes and dielectric films are stacked on top of each other. Through ASD, the controlled deposition of calcined ceramic powder slurries is used to produce the thick films. A particular challenge for fabrication of high voltage (> 100 volts) energy storage capacitors is the formation of high quality dielectric layers of thickness greater than 20 μm that have enhanced breakdown strength and electrical energy density. Thus, the controlled synthesis and processing of smaller particle sizes for the powder slurries used in ASD can improve the dielectric film density and enhance electrical breakdown strength leading to a reduction in capacitor volume. In addition, using finer particles can reduce the bulk sintering temperatures, enhance integration of multiple components, as well as enable the use of less expensive electrode materials. Many of the present MLCCs used in DOE DP systems rely on expensive noble metal electrodes such as Pt or Pd. To control the $Ca(Zr_{1-x},Ti_x)O_3$ powder particle size, used in ASD slurries at Sandia, the synthetic variables and processing conditions that influence final properties must be understood.

There are several synthetic routes for the synthesis of calcium based perovskite powders, however, solution routes offer particular advantages in producing powders with smaller particle sizes because they allow for homogenous mixing of cations and reduced temperatures for phase formation. In essence, active powders tend to have better sintering densities. Among other solution synthesis routes available, there are only a handful that have been reported for the synthesis of bulk $Ca(Zr_{1-x},Ti_x)O_3$ [2, 3] and CZ[4-8] and only one report concerning the combustion synthesis of nanocrystalline CZ[9] in comparison to numerous reports on CT materials. Solution routes to bulk CZT and CZ materials include metal alkoxide sol-gel[2, 5], combustion[7, 10], citrate[3, 6], peroxide[11] and oxalate[4, 5, 8] methods. Some work towards reducing temperatures and particle size for the solid state synthesis of CZ from oxides and carbonates has also been performed using molten salt synthesis[12, 13], mechanochemical activation with vibro milling[14], and high energy ball milling[15]. The mechanochemical routes, however required long milling times (~20 h) or

additional high temperature (900–1100 °C) heat treatments to produce phase pure CZ, while the molten salt synthesis produced powders that were found to include salt impurities. Recently nanocrystalline CZ powders prepared through combustion synthesis were found to reduce the sintering temperature by 150 to 1500 °C and have a density of 98%.[9] This initial demonstration shows the promise of using highly active powders in MLCC devices to enhance performance.

We have begun to explore to the synthesis of controlled particle size powders of $Ca(Zr_{0.90}Ti_{0.10})O_3$, by first synthesizing CZ and CT powders through our patented nonaqueous oxalic acid solution precipitation route to ceramic oxides.[16] This route involves the nonaqueous precipitation of cations with oxalic acid to produce kilogram quantities of a filterable metal oxalate precursor that can be thermally decomposed to the perovskite. This simple synthetic route produces high yield metal oxalate from commercially available precursors (e.g., group (IV) metal alkoxides and metal acetates) and does not require pH adjustments. Our route also differs from reported oxalate methods since it does not rely on the use of metal halides that can lead to halide contamination. Details of the synthesis of CZ and CT powders are discussed below.

2. EXPERIMENTAL PROCEDURES

Precursors. All compounds listed below were used as received: glacial acetic acid (GAA, Fisher); oxalic acid (OA, Acros anhydrous, 98%); acetylacetone (acac, Aldrich); *n*-propanol (*n*-PrOH, Fisher Scientific, certified); calcium acetate ($Ca(O_2CCH_3)_2 \cdot x\ H_2O$, Aldrich lot 03420BT, 99%); calcium oxide (CaO, Fisher lot 751126); calcium carbonate ($CaCO_3$, Alfa Thiokol lot 020384 ultrapure); calcium nitrate $Ca(NO_3)_2 \cdot 4\ H_2O$, (Alfa Aesar Lot 23368, 99.98% metals basis & Spectrum Chemicals, Lot 49132D4, assumed as 99%); titanium(IV) n-butoxide ($(Ti(OBu^n)_4$ or $Ti(O(CH_2)_3CH_3)_4$, Alfa Aesar, a Johnson Matthey Co, 99+); and zirconium(IV) *n*-butoxide ($(Zr(OBu^n)_4$ or $Zr(O(CH_2)_3CH_3)_4$, Fisher).

Calcium Precursor Evaluation. Following the patented route to PZT and other related oxides, this process required the selection of a suitable Ca precursor for reaction with group (IV) *n*-butoxides, GAA, acac, OA, and *n*-PrOH.[16] Several precursors were initially evaluated for their solubility and reactivity within our system. These included $Ca(O_2CCH_3)_2 \cdot x\ H_2O$, CaO, $CaCO_3$, and $Ca(NO_3)_2$. Of the precursors examined, $Ca(NO_3)_2 \cdot 4\ H_2O$ was selected for its solubility in *n*-PrOH as well as maintaining a stable solution (i.e., no precipitate formation) upon reaction with the metal alkoxides.[17] The synthetic process using $Ca(NO_3)_2 \cdot 4\ H_2O$ to produce CT and CZ powders are described below.

Calcium Stock Solution Preparation. Several Ca stock solutions were prepared by first dissolving $Ca(NO_3)_2 \cdot 4\ H_2O$ in *n*-PrOH at 97 °C for 0.5–2.5h with [Ca] = 4.0–5.2 wt. %. The cooled slightly turbid solutions were then filtered with 0.45 or 0.8 μm membrane filters. PXRD pattern from the insoluble residue collected on the membrane filter could not be identified by database. The final solution was then assayed to determine the $[Ca^{2+}]$. Table 1 summarizes the properties of the stock solutions used for CZ and CT powder syntheses.

Table 1. $Ca(NO_3)_2$ stock solutions for CZ1–CZ6.

Stock Soln (ID)	(Wt.%) Ca	Calculated $[Ca^{2+}]$ = Mol Ca/g soln	Assayed $[Ca^{2+}]$= mol Ca/g soln
A	5.20	0.00130	----
B	4.03	0.00101	----
C	4.06	0.00101	0.00104
D	4.01	0.00102	0.00104

$Ca(NO_3)_2$ Assay Procedures. The calculated $[Ca^{2+}]$, listed in Table 1, was determined from the moles of Ca calculated from $Ca(NO_3)_2 \cdot 4\ H_2O$ used in the dissolution and the final solution weight. Assays were performed in triplicate and used alumina crucibles fired to constant weight. Two procedures were followed:

1) ***Stock solution C***. A weighed Ca solution was air dried to form a white crystalline powder in a crucible. The powder was calcined at 1000 °C for 2.5 h and cooled to 550 °C. The crucible was removed from the furnace and cooled to room temperature in a N_2 purged

desiccator to prevent carbonate phase formation. Final calculations indicated that the $[Ca^{2+}]$ = 0.00104 moles/g solution. The XRD pattern of the calcined powder was identified as phase pure CaO.

2) ***Stock solution D***. A weighed amount of Ca solution was placed into a crucible. An OA solution (*n*-PrOH, 20% xs OA) was added, forming a white precipitate. The precipitate was air dried overnight, then heat treated at 50 °C on a hotplate. The powder was calcined at 1000 °C for 2.5 h and cooled to 550 °C in air. The $[Ca^{2+}]$ = 0.00104 moles Ca/ g Ca solution. The XRD pattern of the calcined powder indicated a mixture of $CaCO_3$ and CaO.

General CZ and CT Synthetic Process. Figure 1 illustrates the general synthetic process used for CZ. A similar approach was also used for CT by substituting $Ti(OBu^n)_4$ for $Zr(OBu^n)_4$. This approach involves producing two separate precursor solutions (Zr and Ca) that are mixed to form a homogenous cation solution referred to as the 'metals solution'. To co-precipitate the cations out of the metals solution, it was pumped into an OA/*n*-PrOH solution while shear mixing was underway. The resulting metal oxalate precursor slurry was aged for 1h. Finally, the metal oxalate precursor was collected by filtration, dried, and calcined. The specific synthetic details and optimizations investigated for the CT and CZ powders are described below.

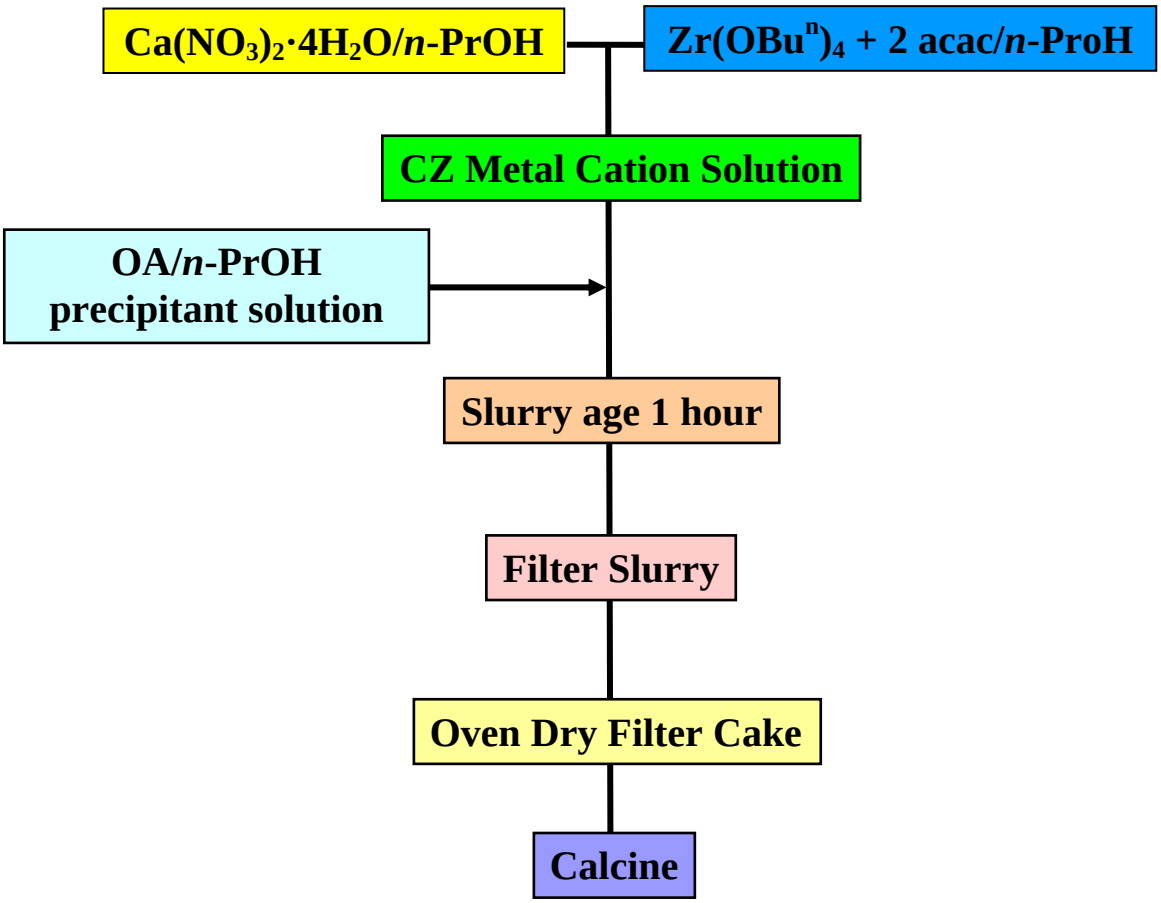

Figure 1. Flowchart of the CZ synthetic process.

General CZ Metal Solution Preparation. The synthetic process used for the CZ metal solutions (CZ1–CZ6) is shown in Figure 2. First, $Zr(OBut^{n})_4$ was diluted with n-PrOH to produce a 50–56 wt.% solution that was reacted with varying amounts of acac for 35 min. A second $Ca(NO_3)_2$/*n*-PrOH solution was also prepared, added directly to the Zr/acac/*n*-PrOH solution, and the mixture was stirred for 2 h. Note: for CZ3–CZ6, a quantitative transfer of residual $Ca(NO_3)_2$ was performed by an additional rinse with *n*-PrOH.

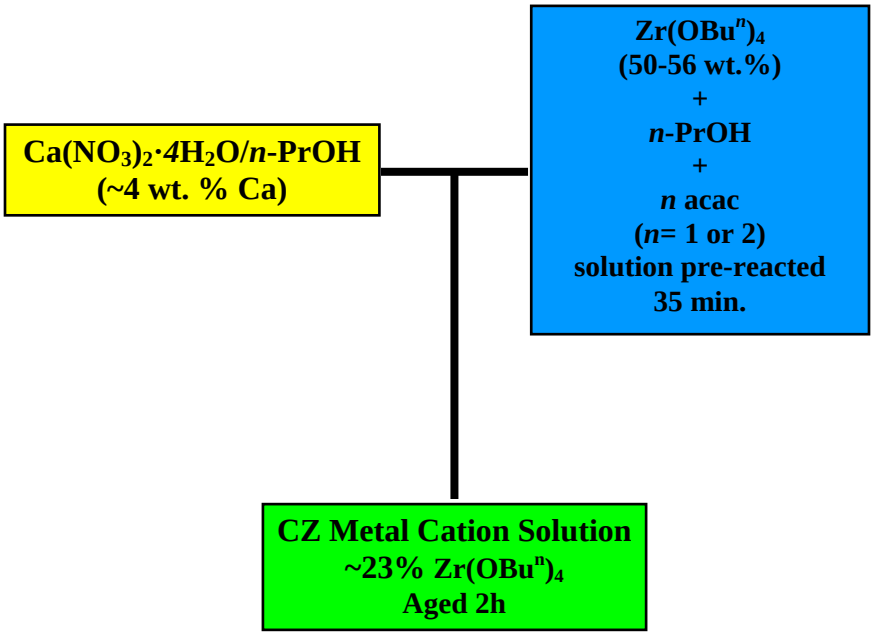

2.
Figure 2. Flowchart for the preparation of the CZ metals solution.

Optimization of acac stoichiometry for CZ. To determine the lowest acac stochiometery that would not inhibit Zr oxalate precipitation, a CZ metal cation solution stability study was conducted. Here, the acac:Zr molar ratios were varied prior to being mixed with the $Ca(NO_3)_2$ solution. Table 2 summarizes the results. The metals solution did not gel or precipitate when ratio 1:1 was used. Final CZ powder batches were synthesized from ratios of 1:1 and 2:1 mol acac/mol $Zr(OBu^n)_4$.

Table 2. CZ metals solution acac:Zr optimization

acac : $Zr(OBu^n)_4$	Pre-reaction time (min) $Zr(OBu^n)_4$ + n-PrOH + acac	Solution Observations after Reacting with $Ca(NO_3)_2$/n-PrOH
0 : 1	0	Gelled Immediately
0.25 : 1	47	Gelled Immediately
0.50 : 1	42	After 45 min, solution is v. sl. turbid; turbid gel overnight (no solid ppt)
1 : 1	36	Solution stable over weekend

CT and CZ Powder Synthesis.

CZ scoping batch*:* A 2 g CZ batch was synthesized using a 1:1 acac:Zr ratio (Table 2). The CZ metals solution was aged for 90 h prior to being added to solution of 17.7 wt. % OA/n-PrOH (3.2 mol OA/mol CZ oxide). The resulting white oxalate slurry was smooth, creamy and gelatinous. Filtration of the 40 mL slurry, in medium frit funnel, took 1.8 h. The collected filter cake was dried at 60–80 °C for 2 days. The dried filter cake was ground up with a mortar and pestle prior to calcination at 750 °C for 1 h. The filtrate was ashed (1000 °C, 2 h) and no residue was collected indicating a complete precipitation of the cations.

Batches: CZ1–CZ6. Based on the results of the scoping batch, the synthetic process illustrated in Figure 1 was developed and used to investigate the reaction condition variables on the final powder properties. Table 3 summarizes the experimental parameters used to synthesize six powder batches (CZ1–CZ6) of $CaZrO_3$. Varied parameters include: batch size, mixing conditions used during co-precipitation, Ca stock solutions, wt% of OA/n-PrOH, acac:Zr stoichiometery, metals solution addition rate, and slurry age. The filtering and drying conditions for these reactions are found in Table 4.

Optimization of conditions used for the 2 g scoping batch was pursued to improve the properties of gelatinous slurry observed. This characteristic is undesirable since it results from inadequate mixing during precipitation and prevents simultaneous homogenous precipitation of Ca^{+2} and Zr^{+4}. The formation of gels can also increase the final particle size and increases time of filtration. To avoid gel formation, shear mixing was used for CZ1, 2, 5 and 6 to improve agitation, dispersion, and reduce particle size. Two shear mixers were employed based on batch size. *Note*: quantitative transfer of residual Ca left in the beaker was made by an n-PrOH rinse Ca for CZ3–CZ6 to improve Ca stoichiometry. Finally, all co-precipitation filtrates for the batches were ashed to determine the % yield of co-precipitants and these results are presented in Table 5.

CZ1 & CZ2. 10 g batches were synthesized using an acac:Zr ratio of 1:1 (CZ1) and 2:1 (CZ2). Ca stock solutions B and C were used respectively. The rotor was operated at a rate of 10,000 rpm while the CZ metals solution was added at 8 mL/min. Upon complete addition of the CZ metals solution, the fluid slurry was shear mixed an additional 5 min. at a rate of 14,000 rpm prior to a 1 h slurry age. Slurries were vacuum filtered in 600 mL medium frit funnels. The cakes were oven dried (Table 4), resulting in dried hard cakes that were ground up with a mortar and pestle prior to calcinations in air.

CZ3 & CZ4. Two 4 g batches were synthesized using an acac:Zr 1:1 ratio (CZ3) and 2:1 (CZ4). Ca stock solution C was used. Due to lower solution volumes, the shear mixer was not used and the resulting slurry was thick and gelatinous. The 1 h aged slurries were vacuum filtered in a 150 mL medium frit funnel in 2 h. The cakes were oven dried (Table 4), resulting in hard cakes that were ground up with a mortar and pestle prior to calcination in air.

Table 3. CZ1–CZ6 synthetic conditions.

Batch ID	Batch size (g)	Shear mixed	[Ca^{2+}]=mol Ca/g soln, Stock ID	*n*-PrOH rinse for Ca	acac:Zr	(wt%) OA in *n*-PrOH	Metals Soln Add Rate (mL/min)	Slurry Age (h)
CZ1	9.4	Yes*	as calc, 0.00101, **Stock B**	N	1 : 1	9.4	9 pump	1
CZ2	9.6	Yes*	as calc, 0.00101, **Stock C**	N	2 : 1	9.6	9 pump	1
CZ3	4.1	No	assayed, 0.00104, **Stock C**	Y	1: 1	9.4	6 pipet	1
CZ4	4.4	No	assayed, 0.00104, **Stock C**	Y	2 :1	9.6	5 pipet	1
CZ5 (split)	8.0	Yes*	assayed, 0.00104, **Stock D**	Y	2 : 1	8.2	8 pump	(CZ5-1) 1 (CZ5-4) 4
CZ6	35.4	Yes**	assayed, 0.00104, **Stock D**	Y	2 : 1	7.6	13 pump	1

* IKA Works T18 Basic, tool = S18N-19G; working range 10-1000 mL

** IKA Works T50 D 55, tool S 50N-G45 FF; working range 250 mL – 7.5L; 1750 rpm shear rate used.

Pump equipment: Masterflex Drive L/S 7523-20; Masterflexpump head: L/S Easyload 7518-10; Tygon tubing L/S 16

Table 4. CZ1–CZ6 filtering/drying Conditions for CZ oxalate precursor.

Batch ID	Batch size (g)	Filter Cake Formation (min)	Filter Cake Drying [°C (h)] (Conditions)	Volatiles Oven Drying (wt%)
CZ1	9.4	15	83 (3.5); 61 (88)	65.9
CZ2	9.6	13.5	66 °C (17); 90 °C (3 h)	70.4
CZ3	4.1	2.2 h	85 °C (87 h)	80.1
CZ4	4.4	2.4 h, stopped early	85 °C (87 h)	78.2
CZ5-1	4	5.3	85 °C (16 h)	67.8
CZ5-4	4	4.8	85 °C (16 h)	66.7
CZ6	35.4	1.4 h	85 °C (62 h)	69.8

CZ5 Slurry Aging study. The cation stoichiometry and yield of co-precipitation for the slurry at 1 and 4 h was evaluated. An 8 g batch was synthesized with an acac:Zr ratio of 2:1 and the Ca stock solution D. The slurry was divided in half after 5 min of shear mixing. One half (control) was aged for 1 h (CZ5-1) and the balance was aged for 4 h (CZ5-4). Both slurries were filtered in 150 mL medium frit funnels. The cakes were oven dried (Table 4) resulting in hard cakes that were ground up with a mortar and pestle prior to calcination in air.

CZ6. A 35 g batch was synthesized with an acac:Zr ratio of 2:1 and the Ca stock solution D. The CZ metals solution was added at 12 mL/min, an increase from 8 mL/min due to the increased batch size. Because of batch scale, the OA/n-PrOH solution was decreased to 7.6 wt. % OA to optimize volume for the shear mixer configuration. During mixing, the temperature of the slurry reached 51 °C. After aging 1h, the slurry was vacuum filtered in a 1.5 L medium frit funnel. The cake was oven dried (Table 4), resulting in a hard cake that was ground up with a mortar and pestle prior to calcination in air.

Table 5. CZ1–CZ6 % yield of CZ oxalate precipitation.

Batch ID	% yield of ppt
CZ1	99.89
CZ2	99.99
CZ3	99.98
CZ4	99.98
CZ5-1	99.99
CZ5-4	99.97
CZ6	99.82

The wt% losses observed for the dried metal oxalate precursors for CZ1–CZ6, due to calcine, are presented below in Table 6. Several calcine conditions were used and explored to determine phase, morphology, and crystallite size of the resulting powders.

Table 6. Calcine Wt% losses for CZ1–CZ6 oven dried metal oxalate precursors.

Calcine condition [°C (h)]	CZ1	CZ2	CZ3	CZ4	CZ5-1	CZ5-4	CZ6
635 (1)	53.9	60.2	----	----	----	----	----
635 °C (10 h)	57.8; 57.4	62.4; 59.2	55.8	58.1	59.7	59.9	----
800 °C (2 h); 635 °C (1 h)	59.0	64.3	58.2	60.6	61.0	61.7	----
650 °C (54 h)	58.7	61.7	----	----	----	-----	58.3; 57.9
750 °C (1 h)	-----	----	57.7	60.3	----	----	----

CT scoping batch. A 3 g batch was made using a similar process employed for CZ1–2 and substituted $Ti(OBu^n)_4$ for $Zr(OBu^n)_4$. The $Ti(OBu^n)_4$ was prereacted with acac (1:1 acac:Ti) for 15 min prior to being diluted with n-PrOH to 50 wt.%. This Ti solution was added to a $Ca(NO_3)_2$/n-PrOH solution drop wise and aged for 3.3 h to observe the stability of the CT solution. The clear solution was added drop wise by pipette to a stirred solution of 17.7 wt. % OA/n-PrOH (3.2 mol OA/mol CT oxide) that was filtered (1 μm). The resulting slurry was thick, creamy, gelatinous, and yellow in color that was aged for 30 min. A 60 mL medium frit funnel was used and took 1.5 h to filter. The gelatinous and voluminous filter cake was oven dried, resulting in a hard cake that was ground up with a mortar and pestle prior to calcination in air. PXRD of the calcined filtrate ash, not shown, was a mixture of TiO_2 (rutile) and $CaTiO_3$. It was estimated that the reaction was 98.7 wt. % complete. The synthesis of CT was not further optimized.

Ball Milling. A dilute slurry of CZ6 powder in n-PrOH was milled in a plastic bottle containing 3/8 inch Y-stabilized ZrO_2 media for 4 h using a US Stoneware Ball Mill, Model 755 RMV.

Powder X-ray Diffraction (PXRD). Oven dried metal oxalate precursors and calcined CZ and CT powders were mounted directly onto a quartz zero background holder purchased from the Gem Dugout. Phase identification for the nanoscale materials was determined from PXRD patterns collected on a PANalytical powder diffractometer employing Cu K_α radiation (1.5406 Å) and a RTMS X'Celerator detector. Samples were scanned at a rate of 0.02°/2 sec in the 2θ range of 10–100°.

Transmission Electron Microscopy (TEM). An aliquot of the particles dispersed in EtOH was placed directly onto a lacy carbon Type-A, 300 mesh, copper TEM grid purchased from Ted Pella, Inc. The aliquot was then allowed to dry overnight. The resultant particles were studied using a Philips CM 30 TEM operating at 300 kV accelerating voltage and equipped with an energy dispersive spectrometer (EDS).

Thermal Analysis. CZ1 and CZ2 oxalate powders (10–20 mg) underwent thermo gravimetric analysis (TGA) and differential thermal analysis (DTA) on a TA Instruments STD 2960 Simultaneous DTA-TGA. Samples were heated in alumina pans under air at a rate of 3°C/min to 900 °C. For oxalate powders CZ3–CZ6 (10–20 mg), thermal analysis was performed on a Netzsch STA 409 PC instrument at a rate of 3 °C/min to 900 °C in air.

Pellets & Sintering Study. Calcined CZ powders (1.5 g) were mixed with a few drops of 1.5 wt % aqueous solution of both polyvinyl alcohol (MW = 15K) and polyethylene glycol (MW = 20M) binders. After drying, the mixed powders were placed in a 0.5 inch diameter pellet press and placed under 15,000 psi. Pellets were sintered at 1375° and 1400°C for 2 h. The density was measured using Archimedes and geometric methods. The green density of the pellets was fairly low, only 35% of the theoretical value of 4.63 g/cm^3. Linear shrinkage of the pellets, during heating, was measured with an *in situ* high-temperature optical imaging system using a camera and strobe illumination made by Control Vision Inc. in Sahuarita, AZ.

Dielectric Testing. Low field dielectric properties were obtained on fired pellets that were approximately 1 cm in diameter and 1 mm thick. Gold electrodes were sputter deposited onto the CZ pellets to obtain electrical contact. Capacitance and dielectric loss were measured at 1 V rms ac between 20 Hz and 1 MHz using an Agilent 4284A Precision LCR Meter. Monopolar polarization vs. field loops were measured at 10 Hz for electric fields that ranged from 10 to 60 kV/cm using a Radiant Technologies Precision Workstation and Trek 609A 10 kV amplifier.

3. RESULTS & DISCUSSION

3.1. Development of a Large-Scale CT and CZ synthetic Route.

The synthetic process developed for CZ and CT fine powders was based on our patented route to PZT.[16] In this process, a homogenous metal alkoxy acetate solution is precipitated to produce a metal oxalate precursor that is subsequently filtered, dried, and calcined in air. This general process is easily modified to synthesize a wide variety metal oxide materials and we have extended it to include calcium based perovksites, Figure 1. Our modified route uses $Ca(NO_3)_2 \cdot 4H_2O$ instead of calcium acetate or calcium alkoxides but continued to employ group (IV) alkoxides. The rapid hydrolysis and low weight/volume percent of commercial calcium alkoxide solutions along with the insoluble calcium acetate oligmers in room temperature acetic acid, with and without acac, prevented their selection for the development of a large-scale synthesis route to CZ and CT. Instead, $Ca(NO_3)_2 \cdot 4H_2O$ was selected based on a previous report on a metal alkoxide sol-gel route[2] to $Ca(Zr_{1-X},Ti_X)O_3$ powders and since a stable metals cation solution was readily achieved. Our stable metals cation solution was prepared following the procedure illustrated in Figure 2. Due to the limited solubility of $Ca(NO_3)_2 \cdot 4H_2O$ in n-BuOH, n-PrOH was used and required a pre-reaction of the chelator, acac, to $Zr(OBu^n)_4$ in order to reduce hydrolysis. Table 2 summarizes the results for the stoichiometric addition of acac:Zr. A minimal 1:1 ratio was necessary to generate a stable metal cation solution that did *not* form precipitates within 72 h. A similar procedure was also used for $Ti(OBu^n)_4$ in the synthesis of CT powders and revealed a minimum 1:1 ratio was necessary. Our studies finally included a maximum acac:Zr of 2:1 to determine the effects of acac addition on the synthetic route and final products.

After preparation of a stable metals cation solution, the cations are coprecipitated by the addition of an OA/n-PrOH solution. The synthetic conditions used for this process are summarized in Table 3 and Table 5 reports the high yields (~99%) of metal oxalate produced by our route. The filtering and drying conditions, used to collect the metal oxalate precursor, is shown in Table 4. Finally, the precursor powders were calcined, pressed into pellets, and sintered for our studies. Our investigation of the reaction parameters and processing conditions for six samples of CZ: shear mixed and varied acac:Zr (CZ1 & CZ2), no shear mixing and varied acac:Zr (CZ3 & CZ4), slurry aging for a 2:1 acac:Zr (CZ5), and scale up for a 2:1 acac:Zr (CZ6), along with the synthesis of CT are reported. For simplicity, the results for our initial characterization studies using samples from the scoping batch (CZ1 & CZ2) will be presented first followed by a general discussion of CZ3-5, and finally CT.

3.2. Characterization of the Oven Dried CZ Precursor.

X-ray Diffraction. Our initial reactions examined the influence of acac on our solution process and final sintered materials. Solutions were prepared with a 1:1 stoichiometric amount of Ca:Zr. For sample CZ1, an acac:Zr ratio of 1:1 was used while CZ2 had a 2:1 ratio. The amorphous precipitated precursor generated from these solutions was filtered and oven dried, Table 4. It was discovered by XRD, that the drying step induces crystallization of the precursor, Figure 3.

PXRD of our oven dried oxalate precursor inferred the crystallization of a double metal oxalate hydrate ($Ca|Zr(O_2C_4)_3|\cdot H_2O$). Analysis of the pattern, using the literature and XRD database[18], indicated that it could be fit by two files—one generated by a dicalcium zirconium oxalate hydrate ($Ca_2Zr(C_2O_4)_4\cdot 5H_2O$, PDF # 01-072-9960)[8, 19, 20] and one generated by ($Ca|Zr(O_2C_4)_3|\cdot H_2O$, PDF # 00-048-1183).[5] Unidentified reflections in our pattern are denoted with an (*) in Figure 3. These unidentified reflections might result from the amount of H_2O present in our CZ samples.[19, 20] For example, the first database pattern, of $Ca_2Zr(C_2O_4)_4\cdot 5H_2O$, was produced from single crystals synthesized from the controlled diffusion of Ca^{2+} and Zr^{4+} through silica gel impregnated by OA. HTXRD on the reported $Ca_2Zr(C_2O_4)_4\cdot 5H_2O$ pattern found that splitting of reflections for $2\theta > 30°$ occurred when heated to 100 °C and the CZ oxalate deyhydrated.[8] The observed phase generated for CZ oxalates may also have a large solubility range for various Ca:Zr stoichiometries. For the second similar pattern, a low temperature crystallization of a calcium zirconium oxalate hydrate ($Ca|Zr(O_2C_4)_3|\cdot H_2O$, PDF # 00-048-1183) was reported.[5] This product was crystallized at 105 °C from the aqueous co-precipitation of $ZrCl_4$ and $CaCl_2$ with oxalic acid, and despite induced stoichiometric changes in Ca:Zr of 1:1 to 1:4 during solution synthesis—the same crystalline phase was always observed. Thus, this phase may have a large solubility range for both Ca^{2+} and Zr^{4+} cations. Finally, a calcium zirconyl oxalate hydrate $CaZrO(C_2O_4)_2\cdot 5H_2O$ from $ZrOCl_2\cdot 8H_2O$ and $CaCl_2$, prepared from $CaCO_3$ has also been suggested based on wet chemical analysis.[4] Since we used a Ca:Zr of 1:1 during the synthesis, it was expected that our $Ca|Zr(O_2C_4)_3|\cdot H_2O$, which we will refer as, CZ Ox maintained this stoichiometry.

The synthetic conditions explored, in all the routes, did not significantly change the crystalline CZ Ox phase produced. Figure 4 shows the XRD patterns for all of the CZ samples prepared in this study. It appears that the drying conditions used (Table 4) slightly changed the reflection intensity; whereas acac:Zr ratios (CZ1–CZ6), shear mixing (CZ1–2), aging of the oxalate slurry (CZ5), or scale-up effects (CZ6) had minimal effect XRD peak intensities. The drying conditions may have altered the levels of hydration too. Although the actual elemental composition and hydration were not determined for these powders, thermal analysis on all of our precursor powders also confirms the production of a CZ oxalate hydrate with 1:1 stoichiometry.

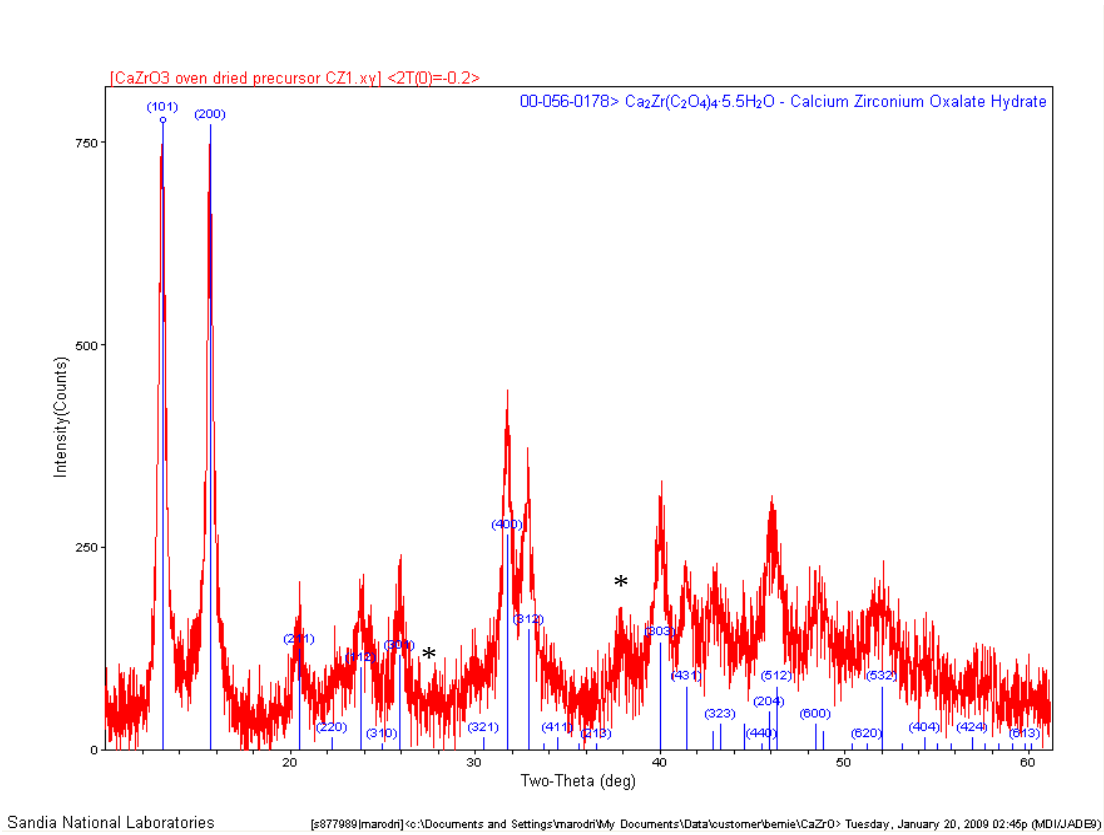

Figure 3. XRD of oven dried CZ1 Ox and best fit index ($Ca_2Zr(C_2O_4)_4 \cdot 5.5H_2O$, PDF # 00-056-0178, calcium zirconium oxalate hydrate).

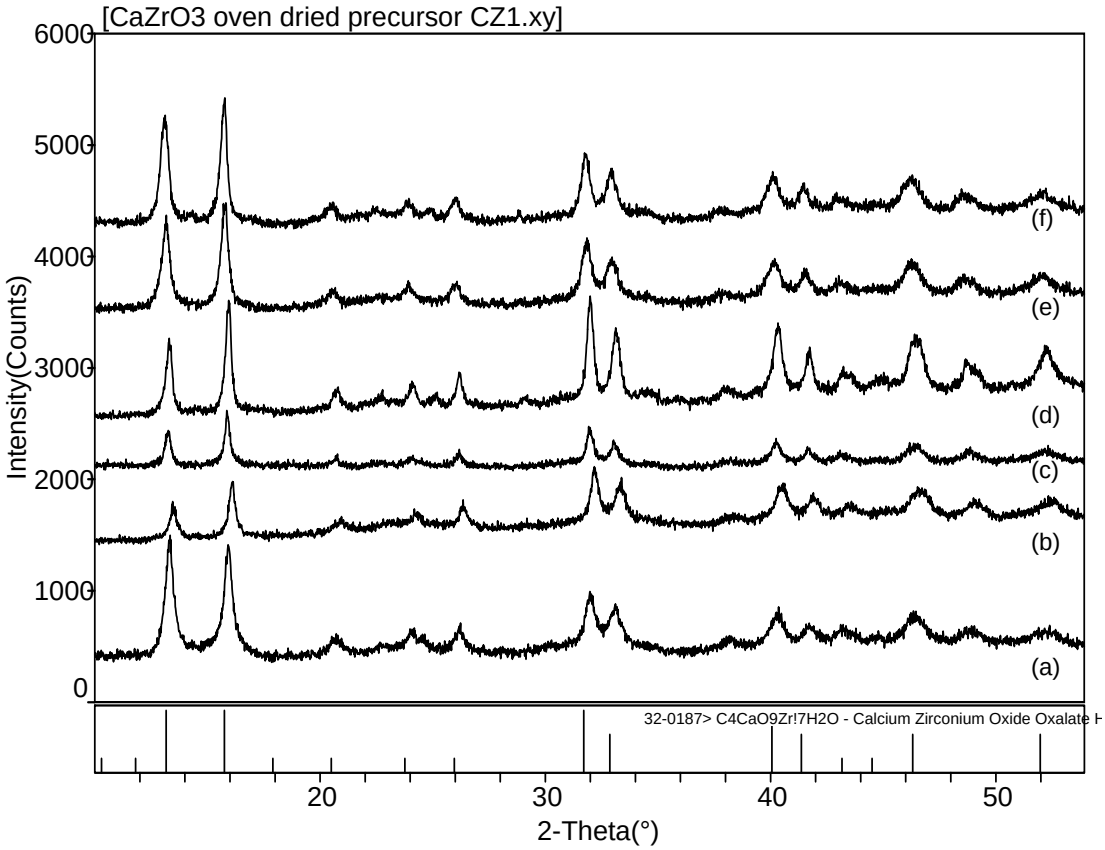

Figure 4. XRD of oven dried CZ Ox for (a) CZ1, (b) CZ2, (c) CZ3, (d) CZ4, (e) CZ5-1, (f) CZ5-4, and (g) CZ6.

Thermal Analysis. TGA/DTA was used to determine decomposition and crystallization behavior of our CaZr oxalate hydrate (CZ Ox). Since two instruments were used, the TGA/DTA for CZ1 and CZ2, are shown in Figures 4 while the compiled data for the remaining CZ samples are shown in Figure 5.

The CaZr Ox decomposes in air in three stages to produce two crystalline phases ($Ca_{0.5}Zr_{0.5}O_{1.5}$ and $CaZrO_3$). Figures 5 and 6 demonstrate that the decomposition of the CZ Ox precursors are completed by 800 °C with a weight loss of 59–64% observed by 900 °C. XRD on CZ1 and CZ2 powders after thermal analysis are shown in Figure 7f and 8f, respectively. The observed weight losses for our CaZr Ox at 900 °C into the $Ca_{0.50}Zr_{0.50}O_{1.5}$ fluorite and orthorhombic $CaZrO_3$ phases detected by XRD are close to the theoretical weight loss of 65% reported from the decomposition of $Ca|Zr(O_2C_4)_3|\cdot H_2O$. Table 6 shows the calcine wt% losses for all CZ powders under several conditions, which are also in range of the calculated value and phases detected. Theoretical weight loss calculations, based on $Ca_2Zr(C_2O_4)_4\cdot 5H_2O$ and the phases present by PXRD patterns, were 44% and thus omitted the oxalate compound from discussion. This assignment was also abandoned because $Ca_2Zr(C_2O_4)\cdot 5H_2O$ has been shown to decompose into $CaZrO_3$ and CaO at similar temperatures.[8] Our CaZr Ox precursor decomposes in three stages that have been proposed for other CZ oxalates.[4, 5, 21] These stages include two dehydration steps (25–260 °C), oxalate decomposition (290–400 °C), and carbonate decomposition (>400 °C).

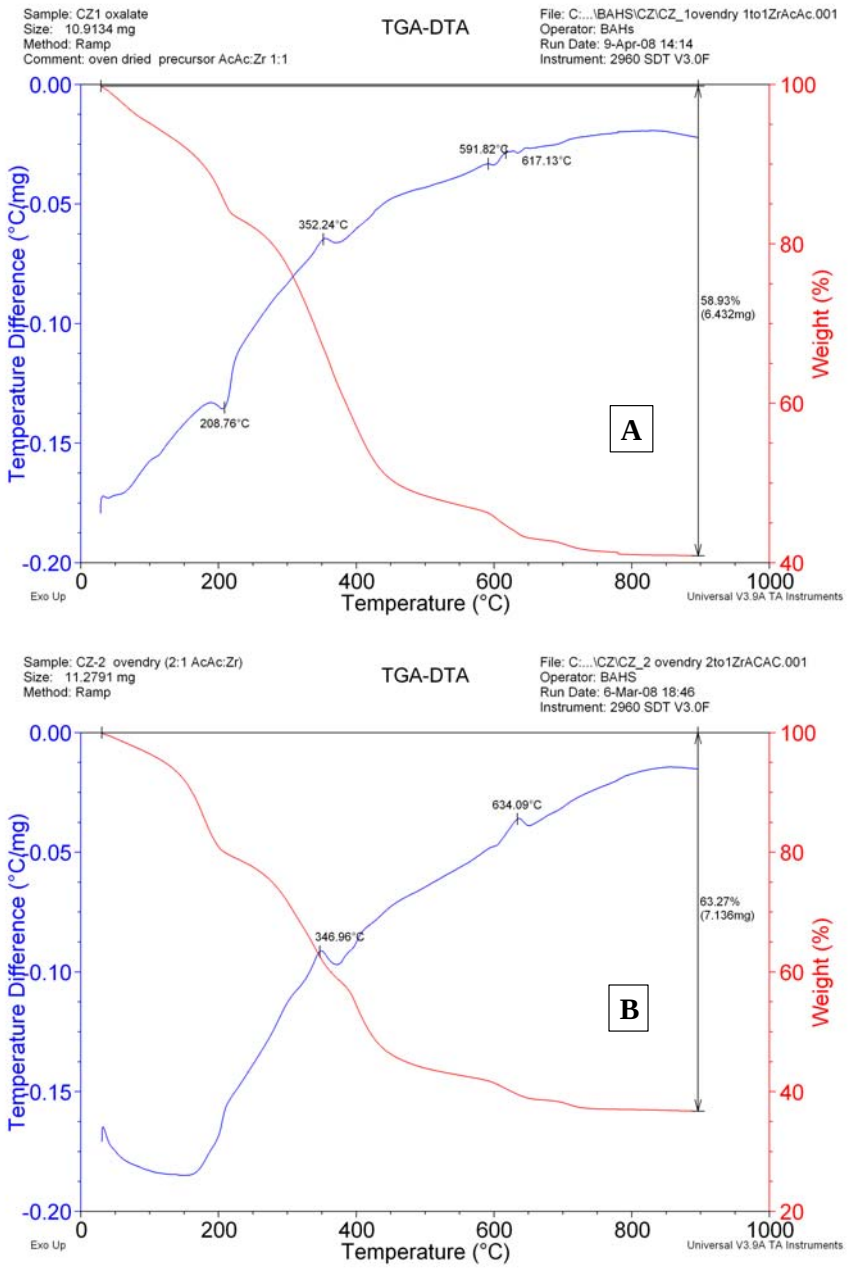

Figure 5. TGA-DTA plots of oven dried CZ Ox for (a) CZ1 and (b) CZ2.

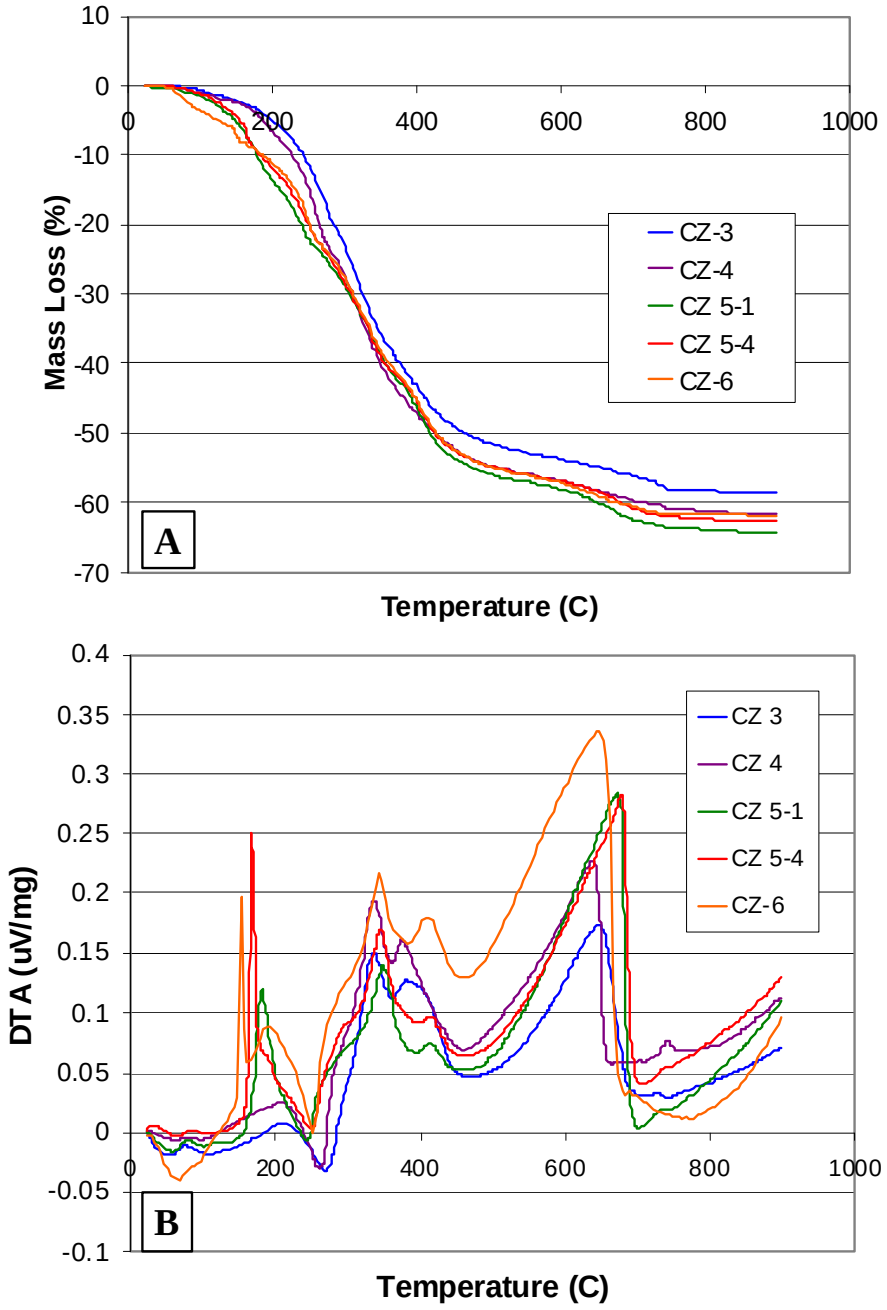

Figure 6. TGA/DTA plots of oven dried CZ Ox for CZ3–CZ6.

The thermal plots compare the effects of acac:Zr ratios (CZ1–CZ6), shear mixing (CZ1, 2, 5, 6), oxalate slurry aging (CZ5), and scale-up effects (CZ6) on decomposition. The amount of water or other organics removed during oven drying is the most apparent difference for the 100–260 °C region in all the samples. The varying exotherms for the second stage of dehydration for slurry age (CZ5-1 & CZ5-4) and scale up (CZ6) may have resulted from drying conditions used, Table 4. These batches had up to 66–69% wt% loss in volatiles vs. ~80% for CZ3&4 after oven drying. The onset of oxalate decomposition has also changed slightly (~220–250 °C). Finally, the formation of the fluorite phase $Ca_{0.50}Zr_{0.50}O_{1.5}$ appears to form at a lower temperature for

powders prepared with an acac:Zr ratio of 2:1, even for the larger scale (CZ6). HTXRD was not performed on the oven dried precursor and therefore phase assignments are based from analysis on various heat treatments, Figures 6–8. These phases identified are discussed next.

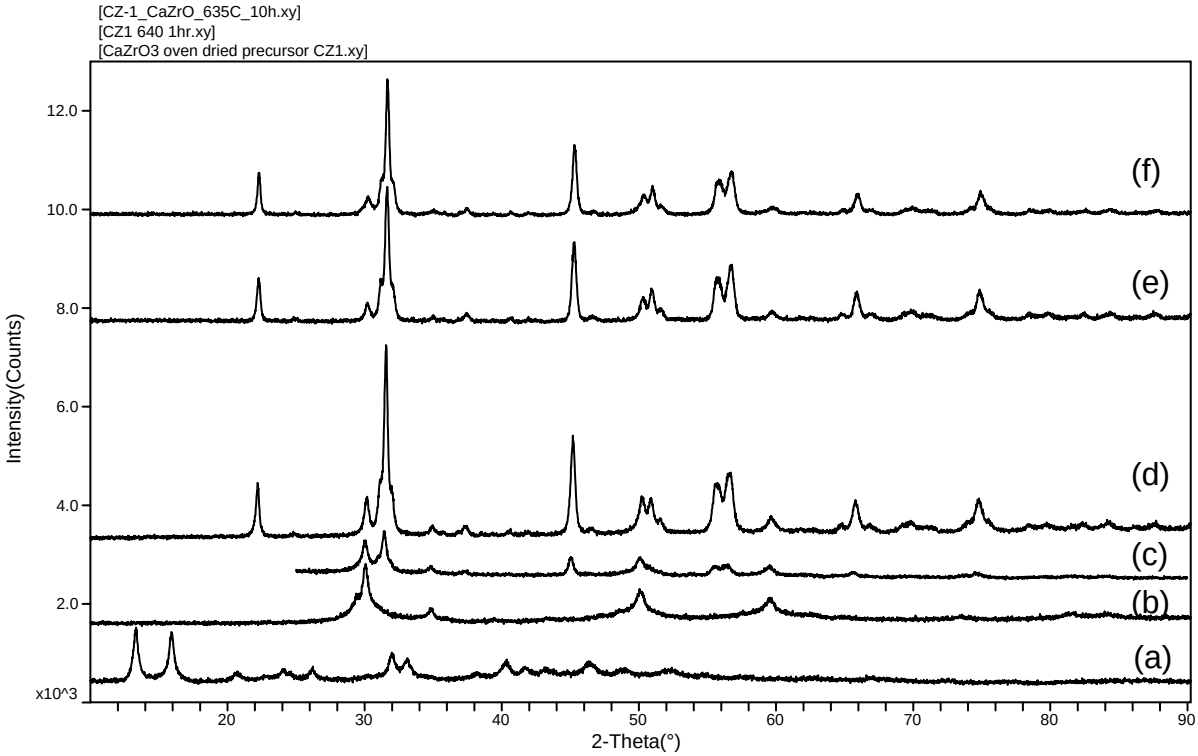

Figure 7. CZ1 XRD comparison: (a) oven dried, 90 °C, (CaZr Ox); (b) calcine 650 °C, 1h, ($Ca_{0.50}Zr_{0.50}O_{1.5}$, fluorite), (c) calcine 650 °C,10h (fluorite & $CaZrO_3$); (d) calcine 650 °C, 54 h, (fluorite & $CaZrO_3$), (e) calcine 800 °C, 2h (fluorite & $CaZrO_3$), and (f) TGA/DTA 900 °C (fluorite & $CaZrO_3$).

3.3. Characterization of the Oven Dried CZ Precursor.

XRD on calcined powders indicates that the CZ Ox converts to a $Ca_{0.50}Zr_{0.50}O_{1.5}$ fluorite phase and is a precursor to orthorhombic $CaZrO_3$. Various calcination conditions were explored to determine what temperatures were necessary to obtain phase pure $CaZrO_3$ powders before sintering conditions were explored. Figures 6 and 7 reveal the crystalline phases formed for CZ1 & CZ2 from these conditions. At 650 °C, a phase we describe as a $Ca_{0.50}Zr_{0.50}O_{1.5}$ fluorite phase is present, Figure 7b. This phase has been commonly referred in the literature as calcium stabilized zirconia ($Ca_{0.15}Zr_{0.85}O_{1.85}$, calcium zirconium oxide, PDF # 00-26-0341) which has a fluorite related structure and is formed in a variety of solution and solid state synthetic routes.[2, 5, 12, 14, 15] Our initial assignment of this phase was based on $Ca_{0.15}Zr_{0.85}O_{1.85}$; however refinement on our XRD pattern (Figure 9) and comparison of the weight losses observed during thermal analysis indicates that this phase is stoichiometric in Ca:Zr ($Ca_{0.50}Zr_{0.50}O_{1.5}$) based on the refined site occupancies. Data used was from CZ2 and the unit cell parameters for our fluorite phase are listed in Figure 9. Finally, crystallite size of 5 nm was calculated from these data.

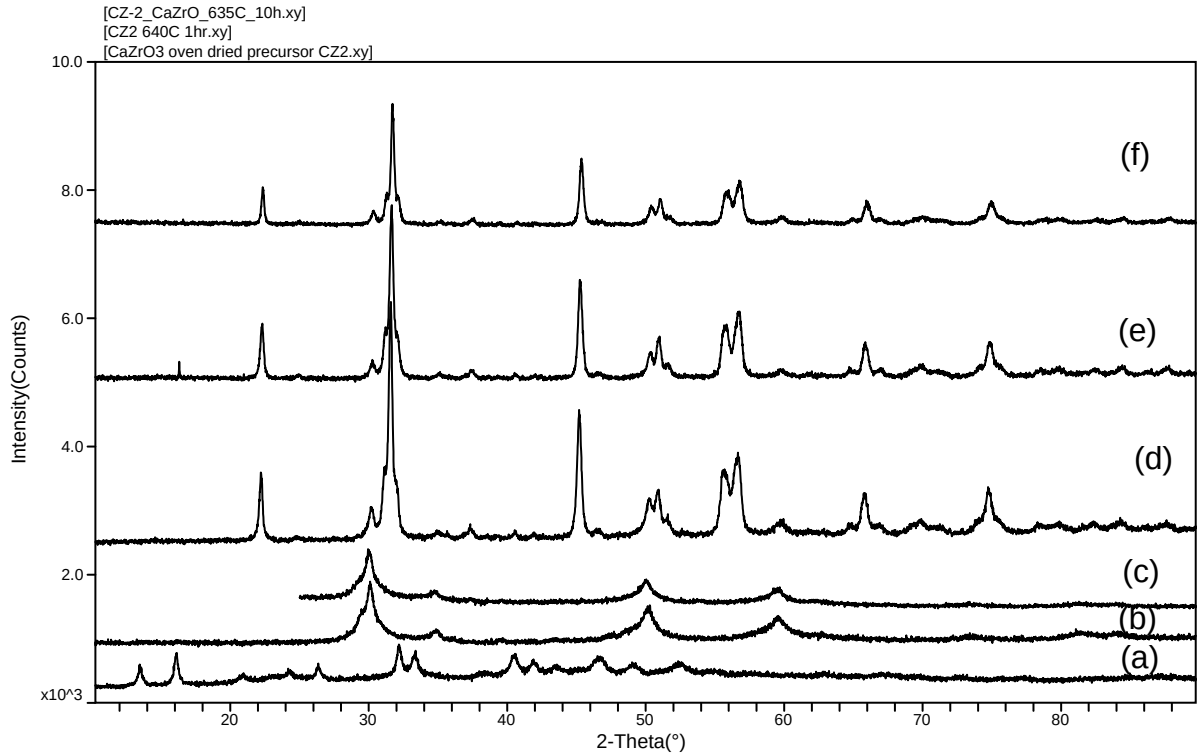

Figure 8. CZ2 XRD comparison: (a) oven dried, 90 °C (CaZr Ox); (b) calcine 650 °C, 1h ($Ca_{0.50}Zr_{0.50}O_{1.5}$, fluorite), (c) calcine 650 °C,10h (fluorite); (d) calcine 650 °C, 54 h (fluorite & $CaZrO_3$), (e) calcine 800 °C, 2h (fluorite & $CaZrO_3$), and (f) TGA/DTA 900 °C (fluorite & $CaZrO_3$).

To verify if tuning our synthetic methods could avoid the formation of $Ca_{0.50}Zr_{0.50}O_{1.5}$ or lessen the amount produced under calcine conditions, we investigated acac:Zr, slurry age and scale. We found that a 2:1 acac:Zr ratio allows a phase pure fluorite to remain after a 10h hold at 650 °C where as 1:1 ratio under the same conditions started to form $CaZrO_3$, Figures7c & 8c, respectively. Slurry aging for 1h (standard) and 4 h, CZ5-1 and CZ5-4, were also examined (XRD not shown). XRD on CZ5-1 & -4, that were calcined (800 °C, 2h + 650 °C), showed that aging had no effect and also produced patterns with the same relative amounts of fluorite and $CaZrO_3$ phases as found in CZ1 & C2 under the same conditions, Figures 7e & 8e. Scale up conditions also did not change the phase transformations at 650 °C, and again produced a mixed phase powder (XRD not shown). It was found later, during our sintering experiments that higher temperatures were needed to crystallize phase pure $CaZrO_3$. It was also observed that certain calcine conditions favored phase pure transformations from the fluorite phase to $CaZrO_3$ over others. Full details on the sintered phases will be discussed after the electron microscopy section.

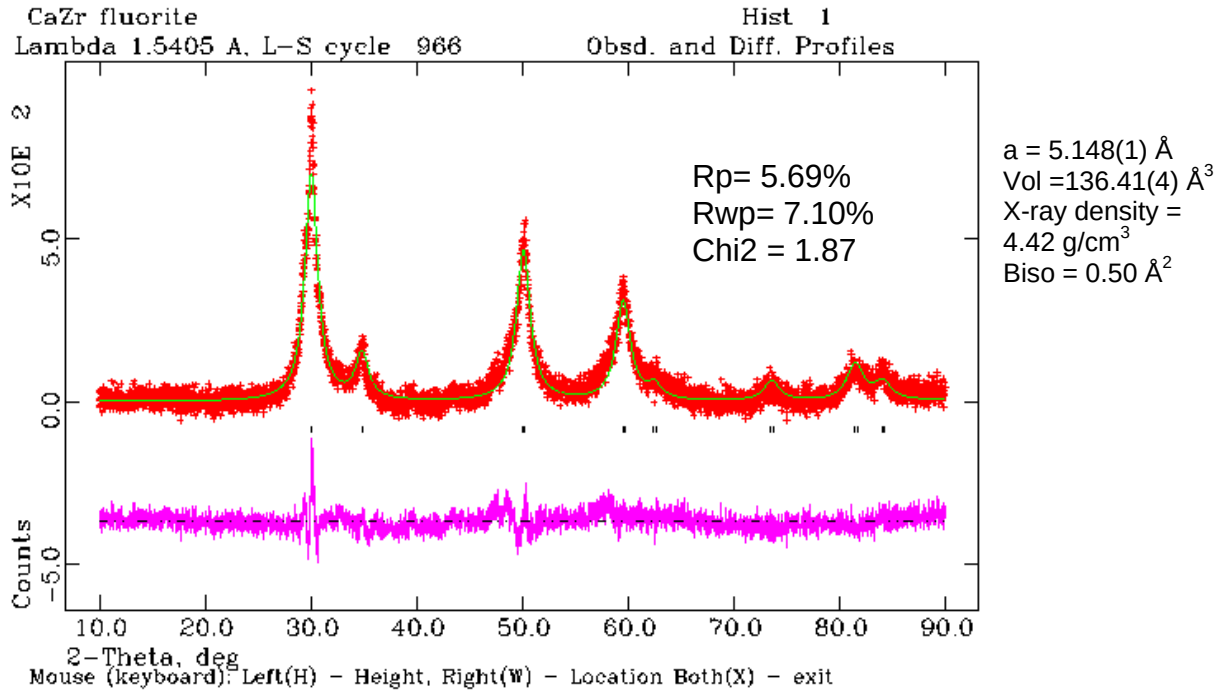

Figure 9. XRD refinement of $Ca_{0.50}Zr_{0.50}O_{1.5}$ fluorite phase, (CZ2 650 °C, 1h.)

Electron Microscopy. Images of the calcined powders revealed that the non-aqueous oxalic acid route and acac:Zr ratio influences low temperature particle morphology. A review of aqueous oxalate co-precipitation routes to $CaZrO_3$,[4, 5] In doped $CaZrO_3$,[22, 23] and calcium stabilized zirconia[24], do not mention any changes in particle morphology. TEM of CZ1 and CZ2, Figure 10, calcined at 635 °C for 10 h showed two distinct particle morphologies. CZ1 (acac:Zr of 1:1) had both "urchin" and "dot" like particle morphologies, while CZ2 (acac:Zr of 2:1) had only urchins. These two morphologies were found to be related to the two nanocrystalline phases observed by XRD, Figures 7c & 8c, respectively.

The composition of the urchins and dots was examined by EDS, Figures 11 and 12. The respective TEM images are also shown. For CZ1(Figure 11), which had both $Ca_{0.5}Zr_{0.5}O_{1.5}$ and $CaZrO_3$ phases, EDS was taken on the center of a cluster of urchins, an isolated urchin and a group of dots. These morphologies were all found to contain both Ca and Zr. The size range for the CZ1 urchin diameters vary from ~0.5–2 μm. An isolated urchin, Figure 11b, illustrates that the spines that nucleate from the center are < 100 nm in diameter. The dot diameters are also on the order of 0.1–0.2 μm. EDS examination of CZ2 (Figure 12), which only had the $Ca_{0.5}Zr_{0.5}O_{1.5}$, also contained Ca and Zr. Figure 12c shows an isolated 50 nm rod from the urchin that is made from smaller crystallites (< 10 nm) which is close to the calculated crystallite size of 5 nm. Quantitative assignments were not made. The observed C signal in the EDS spectra is due to a number of sources not directly related to the nanomaterial's C content (e.g., TEM substrate, contamination buildup, differential absorption of the soft carbon X-rays). SEM images of CZ1

powder, after an additional heat treatment at 800 °C for 2h, are shown in Figure 13. Figures 13b & 13c show that the urchin-like morphologies are still present with ~100 nm spine diameters and are attached to larger irregular shaped particles. Because the XRD pattern of CZ1 at 800 °C shows relatively more broadening of the fluorite phase reflections than $CaZrO_3$, this phase can be attributed to the nanocrystalline urchin spines.

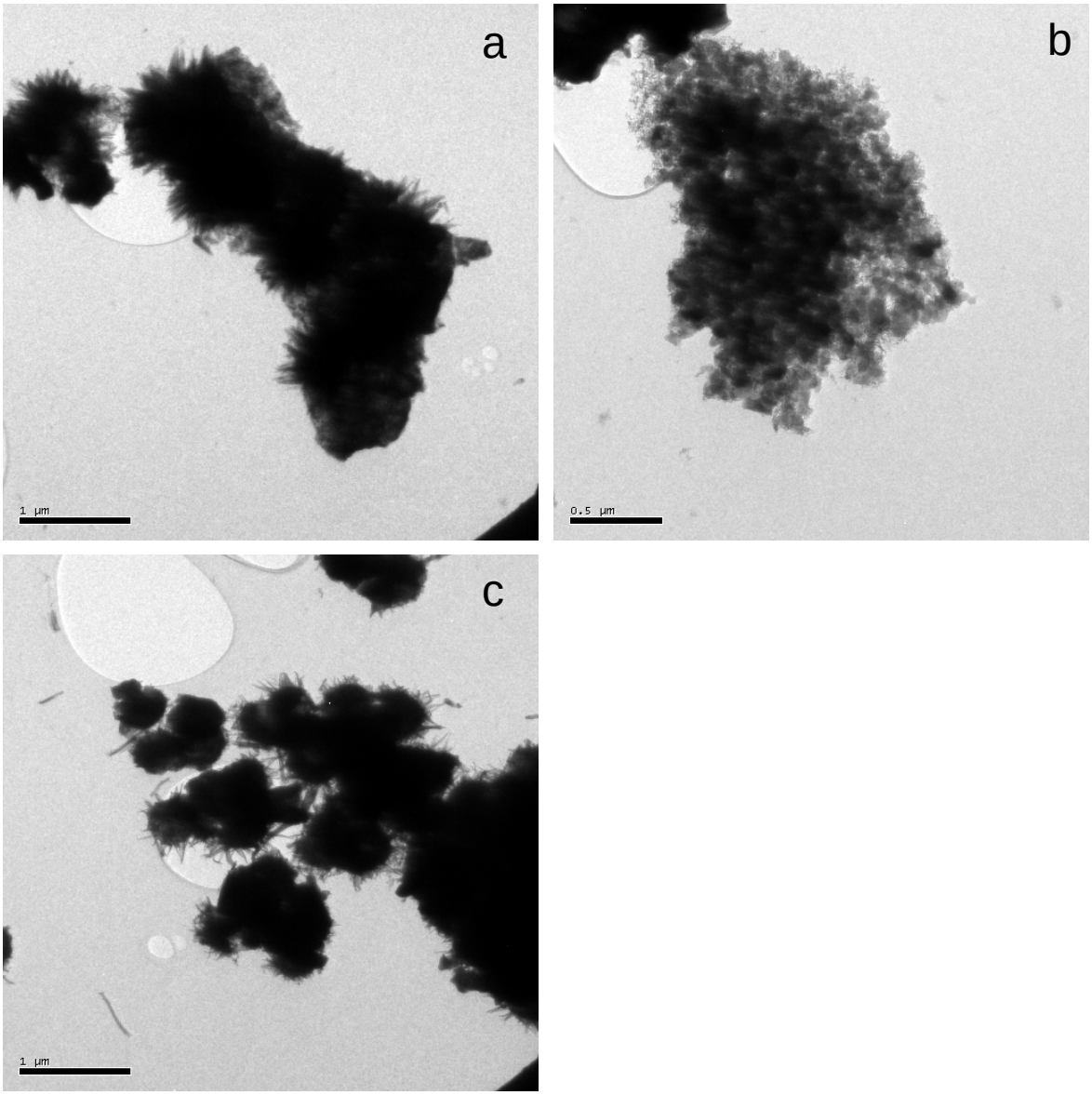

Figure 10. TEM images of CZ1 (635 °C, 10h) (a) urchins, (b) dots and (c) CZ2 (635 °C, 10h) urchins.

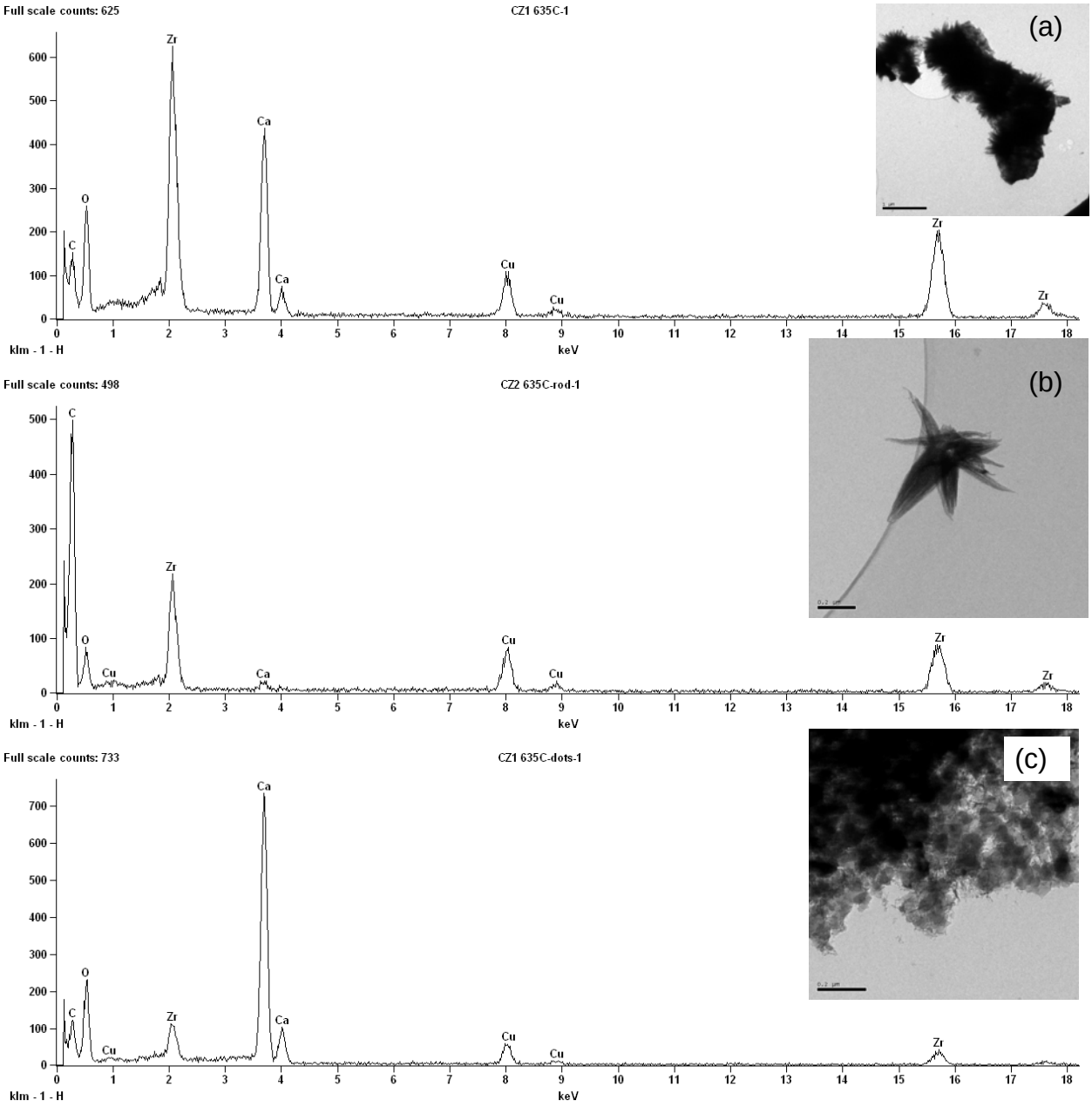

Figure 11. EDS and TEM of CZ-1 (635 °C, 10h). EDS performed on (a) center of urchin (1 μm scale bar), (b) on rod of single urchin (0.2 μm scale bar), and (d) on the dots (0.2 μm scale bar).

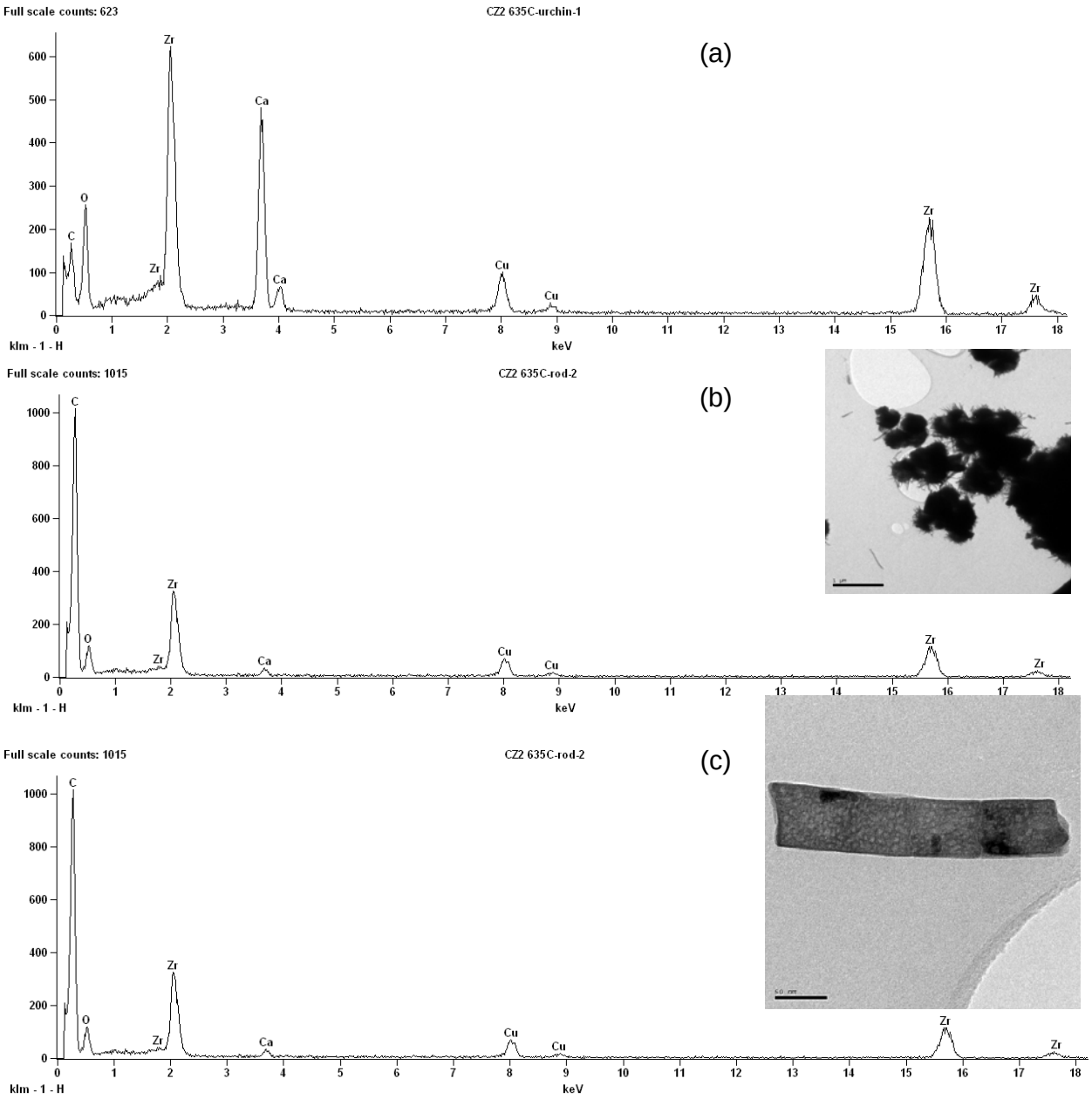

Figure 12. EDS and TEM of CZ2 (635 °C, 10h). EDS performed on (a) center of urchins, (b) edge of urchin rods (1 μm scale bar) and, (c) on single rod (50 nm scale bar).

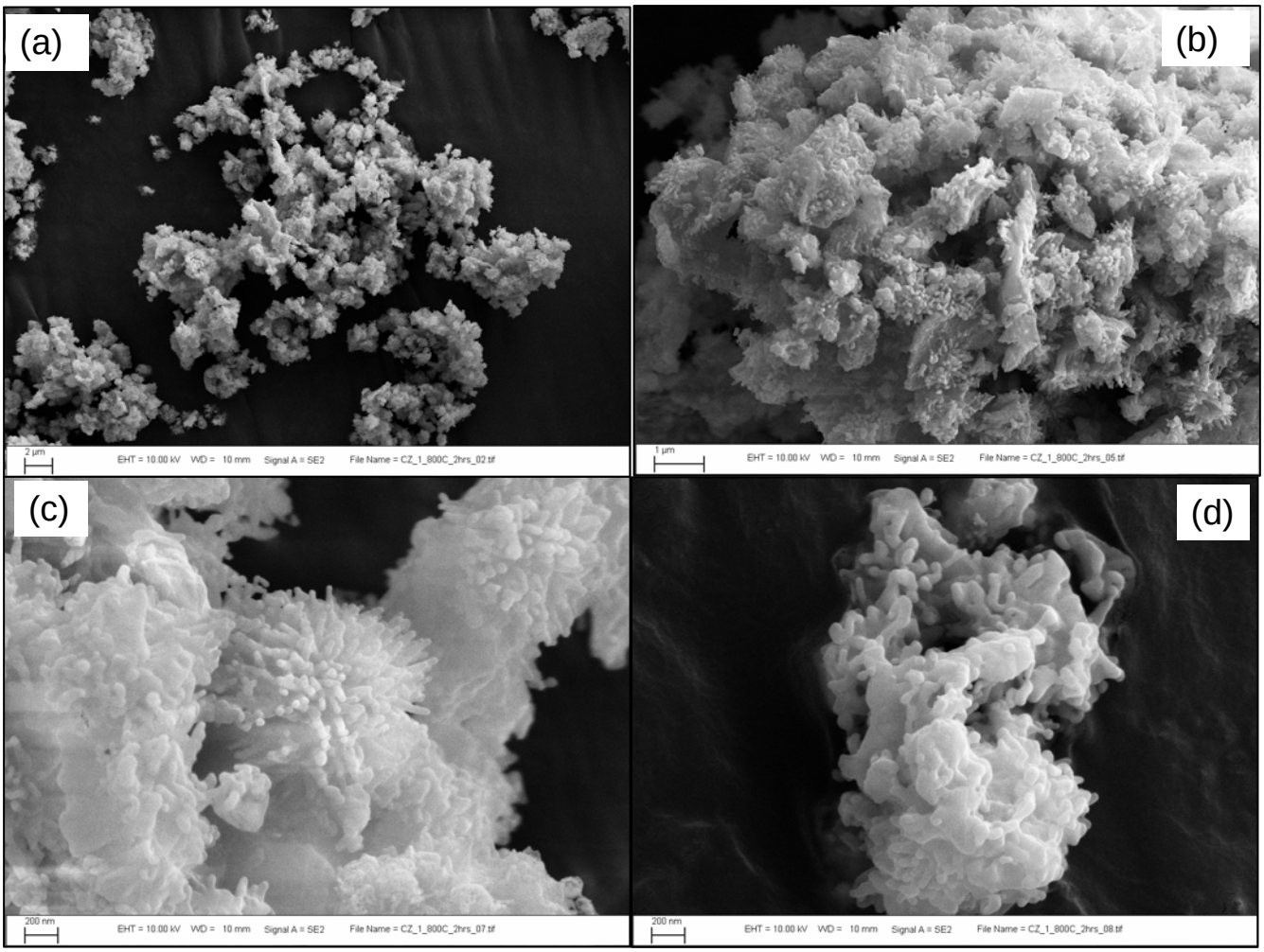

Figure 13. SEM on CZ1 after 1 h at 635 °C + 2 h 800 °C. Scale bar (a) 2 μm, (b) 1 μm, (c) 200 nm, and (d) 200 nm. Urchin like morphology still present. Corresponding XRD is Figure 7e.

3.4. Characterization of Sintered CZ Pellets

To evaluate how our synthetic process controlled the final sintering properties, samples from all 6 batches of CZ were used to produce pellets in order to measure shrinkage, sintering density, and final phase. Table 7 summarizes calcine and sintering conditions used, the final phase obtained, as well as the geometric and Archimedes densities. XRD of CZ1 and CZ2 pellets sintered at 1400° and 1375 °C are shown in Figures 14 –16. Finally, the linear shrinkage data for CZ1, CZ2 and CZ6 is presented in Figure 17.

Since our goal was to enhance sinterability of $CaZrO_3$ by producing highly active powders that could lower sintering temperature from the conventional 1500 °C and improve densification, our pellets were sintered at 1400° and 1375 °C at 2h. First, pellets made from CZ1 and CZ2 powders that were calcined at (a) 635 °C for 1h, (b) 650 °C for 54h, and (c) 800 °C for

2h were compared at 1400 °C, Figures 14 & 15. These results indicate that the acac: Zr ratio and the previous calcine conditions of the powders used led to the formation of different final phases.

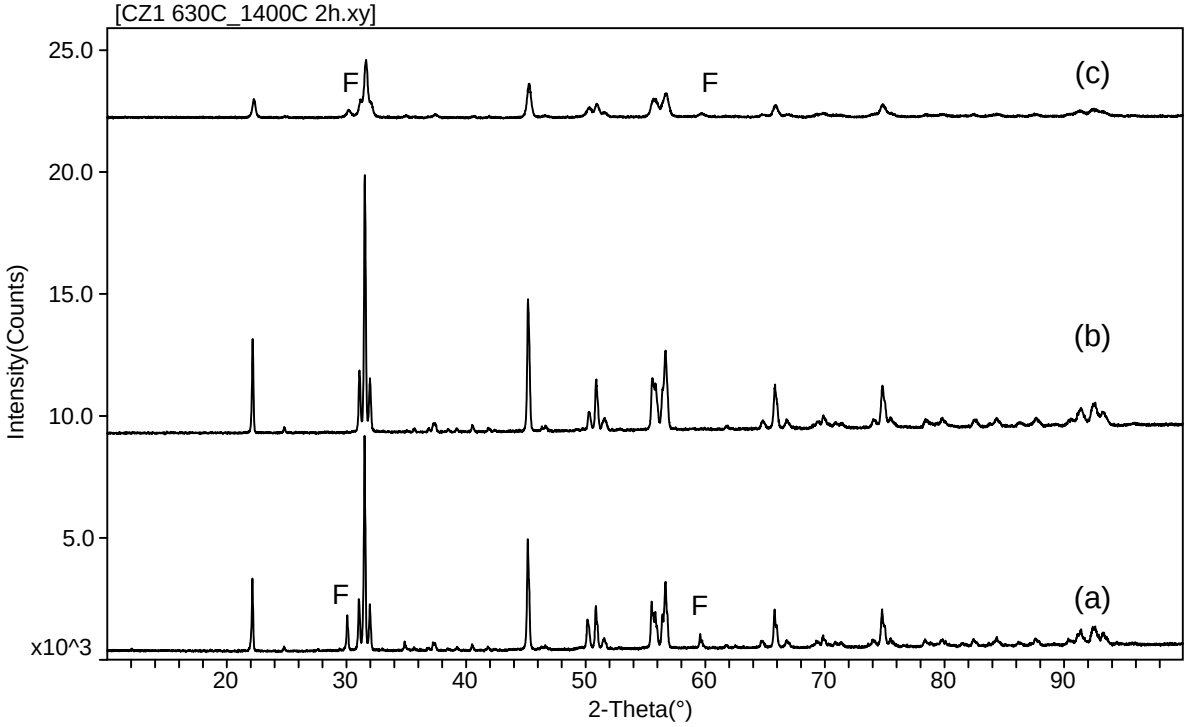

Figure 14. XRD of CZ1 sintered pellets (1400 C, 2h) from powders calcined at (a) 635 °C, 10 h, (b) 650 °C, 54 h, and (c) 635C °C 1h + 800 °C, 2 h. (F = Fluorite)

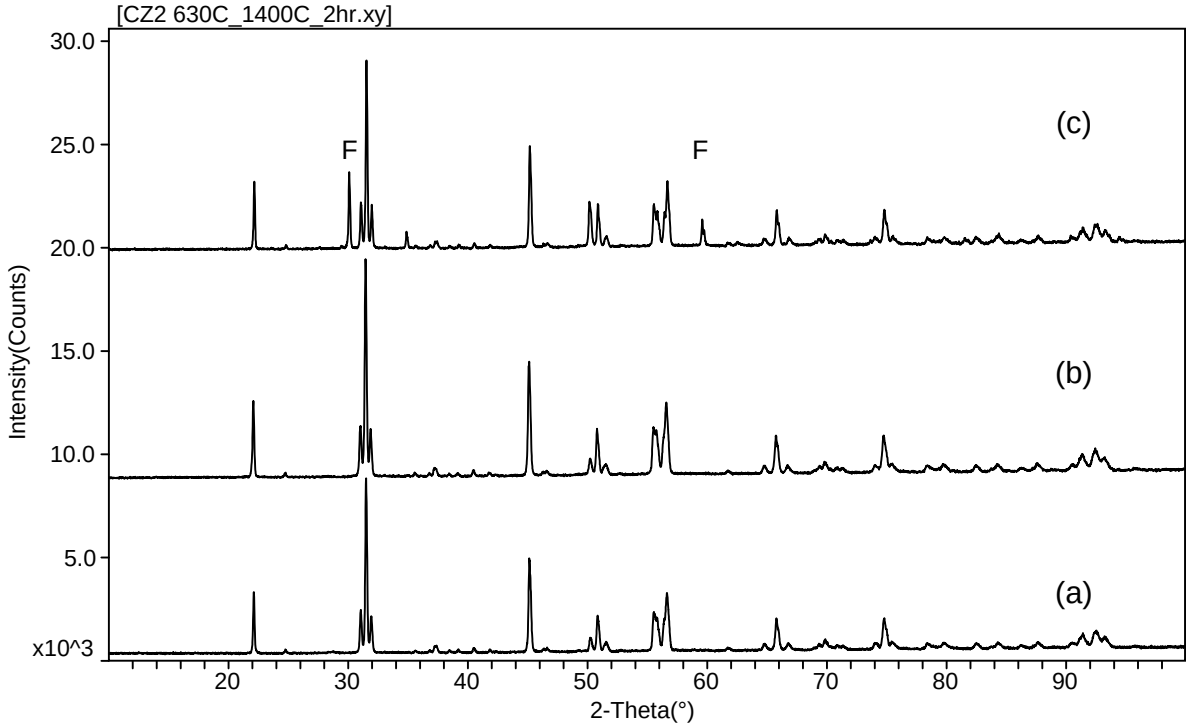

Figure 15. XRD of CZ2 sintered pellets (1400 °C, 2h) from powders calcined at (a) 635 °C, 10 h, (b) 650 °C, 54 h, and (c) 635C °C 1h + 800 °C, 2 h. (F = Fluorite)

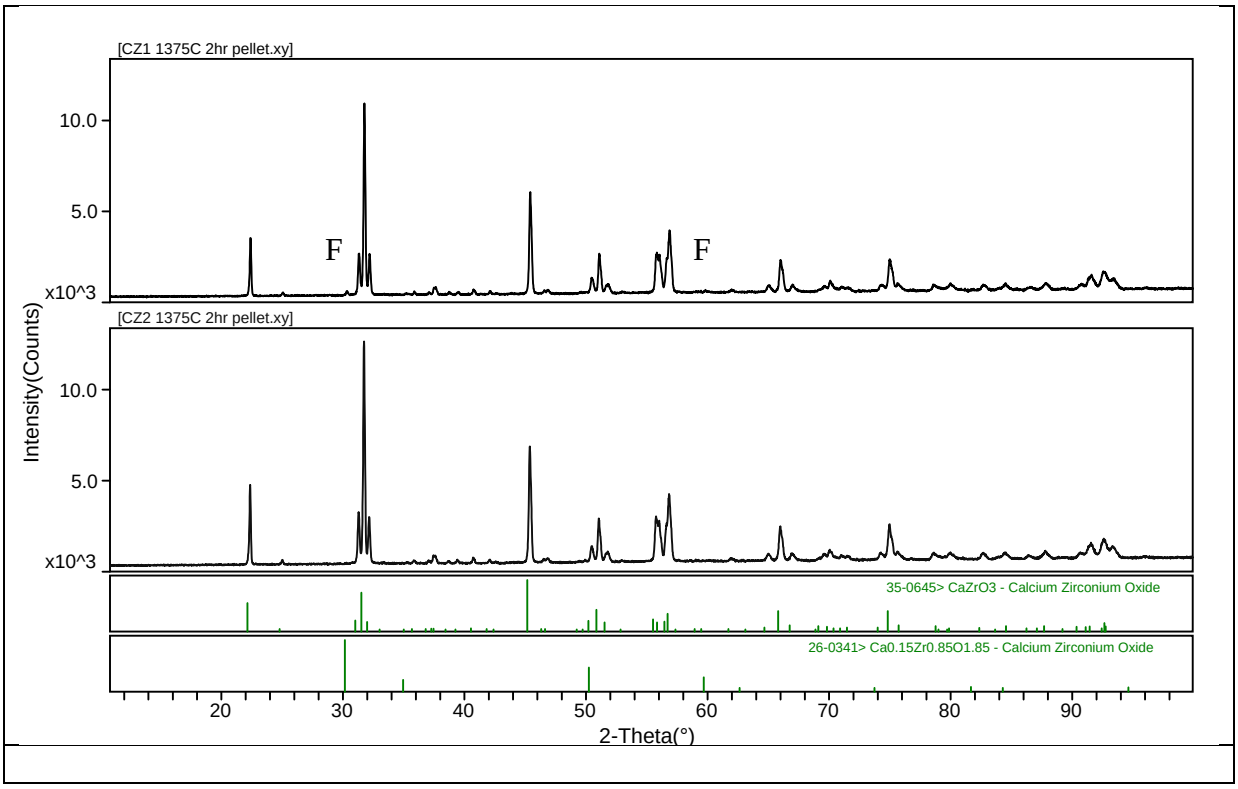

Figure 16. XRD of (a) CZ1 and (b) CZ2 sintered (1375 °C, 2h) from powders calcined 650 °C, 54 h. (F= Fluorite)

We found that the final sintered phases observed demonstrate the importance of using acac and longer calcine hold times to aid in the conversion of the fluorite phase into perovskite $CaZrO_3$ during the sintering process. For example, Figures 14 and 15 show XRD results for CZ1 and CZ2 pellets sintered at 1400 °C for 2h, respectively. $CaZrO_3$ was formed for acac:Zr ratios of 2:1 (CZ2) when powders were previously calcined at ~650 °C (10 and 54h). For the 1:1 (CZ1), only powders calcined at 650 °C (54h) generated $CaZrO_3$. Based on these results, CZ1 and CZ2 pellets were prepared from calcined powders (650 °C, 54h) and sintered at 1375 °C for 2h, Figure 16. Only CZ2 produced $CaZrO_3$. CZ6 (35 g batch) shows the effects of scale up on the final sintered phase and suggests that longer calcine hold time or an initial pyrolysis step may be required. Finally other sintering and calcine conditions were explored, Table 7, which also show that the previous calcine condition is important in generating $CaZrO_3$ during the sintering process. Increasing the calcine temperature but decreasing the hold time did not remove the fluorite phase.

The sintering behavior of the pellets were studied using scale up (CZ6) and different acac:Zr ratios (CZ1 & CZ2) via an *in situ* optical system. The linear shrinkage of pellets made from CZ1, CZ2, and powders calcined at 650 ˚C for 54 h is shown in Figure 17. For CZ6, calcined powders were ball-milled in n-PrOH for 4 h. The pellets heated at 5˚C/min in air had no significant difference in their behavior. All three have accelerated shrinkage after 1200 ˚C. A difference in behavior is observed for the pellets examined during a hold at 1375 °C. CZ6 shrank about 5% more linearly, consistent with reaching near theoretical density as compared to

CZ1 and CZ2. These results suggest ball milling may be necessary to help achieve higher densities at lower sintering temperatures.

Table 7. Pellet sintering conditions used for density measurements. Relative density was calculated using a theoretical density of 4.63 g/cm^3 for orthorhombic $CaZrO_3$. Sintered Phases: (Mixed: F + CZ, Pure: CZ)

Sample	Calcine Condition	Pellet Sintering Condition	Sintered Phases	Geo. Density (g/cm^3)	Arch. Density (g/cm^3)	Relative Density (%)
CZ 1	635C 10h	1400C 2h	CZ + F	2.83		61.1
CZ 1	654C 54h	1400C 2h	CZ			
CZ 1	635C 1 h/ 800C 2h	1400C 2h	CZ + F	3.16		68.3
CZ 1	635C 10h	1375C 2h			3.30	71.3
CZ 1	654C 54h	1375C 2h	CZ+F		3.57	77.1
CZ 1	635C 1 h/ 800C 2h	1375C 2h			3.78	81.6
CZ2	635C 10h	1400C 2h	CZ	3.80		82.1
CZ2	654C 54h	1400C 2h	CZ			
CZ2	635C 1 h/ 800C 2h	1400C 2h		3.19		68.9
CZ 2	635C 10h	1375C 2h			3.47	74.9
CZ 2	654C 54h	1375C 2h	CZ		3.84	82.9
CZ 2	635C 1 h/ 800C 2h	1375C 2h			3.75	81.0
CZ 3	755C 1h	1200C/ 30 min		1.83		39.5
CZ 3	635C 1 h/ 800C 2h	1200C/ 30 min		1.89		40.8
CZ 3	755C 1h	1375C 2h		3.53		76.2
CZ 3	635C 1 h/ 800C 2h	1375C 2h		3.64		78.6
CZ 3	635C 10h	1375C 2h		3.48	3.52	76.0
CZ 4	755C 1h	1200C/ 30 min		1.87		40.4
CZ 4	635C 1 h/ 800C 2h	1200C/ 30 min		1.94		41.9
CZ 4	755C 1h	1375C 2h		3.67		79.3
CZ 4	635C 1 h/ 800C 2h	1375C 2h		3.63		78.4
CZ 4	635C 10h	1375C 2h		3.46	3.42	73.9
CZ 5-1	635C 10h	1375C 2h	CZ+F	4.16	4.09	88.3
CZ 5-1	635C 1 h/ 800C 2h	1375C 2h	CZ+F	4.26	4.27	92.2
CZ 5-4	635C 10h	1375C 2h	CZ+F	4.18	4.16	89.8
CZ 5-4	635C 1 h/ 800C 2h	1375C 2h	CZ+F	4.26	4.38	94.6
CZ 6	650C 54 h	1375C, 2h	CZ+F		4.61	99.6
CZ 6	650C 54 h,ball mill	1375C, 2h	CZ+F		4.34	93.7

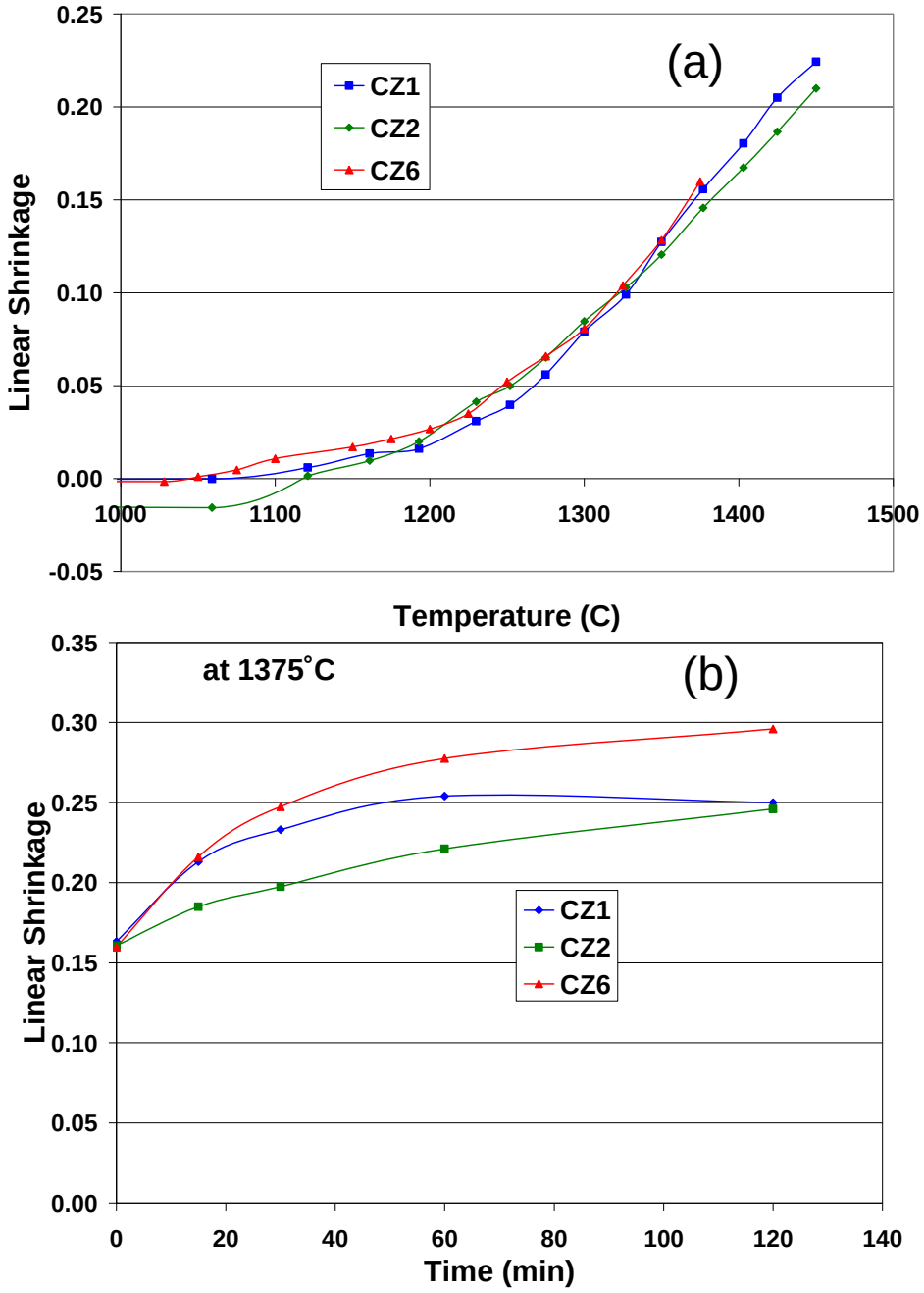

Figure 17. Shrinkage of CZ1, CZ2, and CZ6 in air measured with *in situ* optical system during (a) heating at 5°C/min. and (b) during a hold at 1375 °C. All powders used for pellets in these measurements were calcined at 650 °C, 54h.

3.5. Electrical Characterization of CZ Pellets

Three different types of dielectric measurements were used to electrically characterize chemically prepared CZ pellets. First, low field capacitance and dissipation factor measurements were made on all electroded pellets at ambient temperature (~ 25 ^{o}C) as a function of frequency from 20 Hz to 1 MHz. One volt ac rms voltage was used for these measurements on roughly 1 mm thick specimens, resulting in approximate applied field values of 10 volts/cm. The second electrical test for our samples was monopolar polarization versus field testing at ambient temperature. Electric field values of 10–60 kV/cm in 10kV/cm increments were applied to the samples. These measurements were made to determine if there was enhanced dielectric loss at higher field levels that approach those expected for future component applications. Our final measurement of dielectric constant and dissipation factor was made only on selected samples to confirm the lack of temperature sensitivity in dielectric properties for chem-prep CZ specimens.

Low field, dielectric constant and dissipation factor data are shown in Table 8 for fired ceramic pellets (1375 ^{o}C, 2 h) from several different batches. Encouragingly, our pellets that were single phase perovskite (from batches CZ-1, 2 and 6) had dielectric constants that ranged from 27 to 28.6. Literature values for the dielectric constant of $CaZrO_3$ range from 24.6 to "about" 30.[25, 26] From the classic text book Electroceramics Materials Properties and Applications by A. J. Moulson and J. M. Herbert the extrapolated value for the dielectric constant of 100% dense CZ would be 29.7 ± 0.5.[27] The ± 0.5 range comes from the dielectric constant for CZT 98.5/1.5 being only given to 2 significant figures (K = 29) in the Moulson and Herbert text book. Fired ceramic pellets from batches CZ5-1 and CZ5-4 were found to have second phase fluorite present and exhibited lower dielectric constants than the single phase perovskite batch materials. Dielectric constants of approximately 25 were measured for the CZ5-1 and 4 batch pellets. We also note that the change in dielectric constant with temperature is expected to be extremely small. Recent tests of the dielectric constant of samples fabricated from CZ powder from batch CZ10 powders, which are similar to CZ6 powders, varied by less than 0.8% over a 200 ^{o}C temperature range (-50^{o} to 150 ^{o}C).

A high field polarization versus electric field measurement is shown in Figure 18 for a fired ceramic (1375 ^{o}C/2 hours) that was fabricated from ball milled CZ6 powder. The CZ6 powder was ball milled for 2 h in nalgene jars with zirconia media and propanol. Recent electron microprobe work indicates that no detectable contamination was observed from the yttrium containing Zr milling media. The polarization versus field characteristic was obtained using a 10 ms monopolar, linear ramp voltage that supplied a maximum applied field of 40 kV/cm. There is no hysteresis in the polarization versus field characteristic indicating that this material is low loss at this field level which is 4000 times greater than that used for low field hysteresis measurements. The calculated high field dielectric constant is 31.8 in reasonable agreement with low field values. Polarization values were corrected for the system/holder capacitance of 17 pF that was measured. There may be a slight difference in the measurement of this holder capacitance at low field versus the true holder capacitance at high field. This slight difference in holder capacitance may contribute to the slightly higher high field dielectric constant than expected. Future work will investigate aerosol spray deposited layers for which much higher fields can be applied with our high field polarization versus field equipment (Radiant Technologies Precision Work Station).

Table 8. Low Voltage Dielectric measurements for Sintered Bulk Ceramic CZ Pellets

Sample/ condition	Phase	Relative Density	dia/cm	thick/cm	freq/Hz	Cp/pF	DF	K
CZ-6 no ball mill 650C 54 h, 1375C 2h	CZ+F	99.6%	0.908	0.223	1000	6.96	0.0009	27.1
					10000	6.96		27.1
					100000	6.999		27.2
CZ-6 4 h ball mill 650C 54 h, 1375C 2h	CZ+F	93.7	0.899	0.206	1000	7.71	0.002	28.3
					10000	7.703	0.0002	28.2
CZ5-1 635C 10h, 1375C 2h	CZ+F				1000		0.009	25.2
CZ5-4 635C 10h, 1375C 2h	CZ+F				1000		0.0028	24.9
CZ2 654C 54h, 1400C 2 h	CZ				1000		0.006	27.7
CZ1 654C 54h, 1400C 2h	CZ				1000		0.006	27.7
CZ-1 650C 54 h, 1375C 2h	CZ + F		0.951	0.044	1000	40.83	0.000807	28.6
CZ-2 650C 54 h, 1375C 2h	CZ		0.948	0.036	100	39.66314	0.0022	27.9
					1000	39.27172	0.0026	27.5
					10000	39.19268	0.0013	27.4

Recently, nanocrystalline CZ powders prepared through combustion synthesis were found to reduce the sintering temperature of CZ ceramics by 150 °C to 1500 °C.[9] These ceramics, have a density of 98% and a dielectric constant of 23.8.[9] Through our synthetic routes, we have shown that we can reduce the sintering temperature even further to 1375 °C and obtained a density of greater than 99% for CZ ceramics from our CZ-6 batch powder. Low voltage capacitance data of our pellets indicated that the dielectric constant was approximately 27 for ceramics fabricated from this batch. Our measured dielectric constant values are close to the literature value obtained for $CaZrO_3$ prepared through combustion synthesis. Further, both the dissipation factors (DF) (0.002 to 0.0002) and dielectric constants (27 to 28.3) measured are

also in reasonable agreement with the dielectric constant of 29 and dissipation factor of 0.0003 given by Moulson and Herbert[27] for state of the art commercial $Ca(Zr_{.985}Ti_{0.015})O_3$ powders. This composition is represented by the reduced notation of CZT 98.5 /1.5.

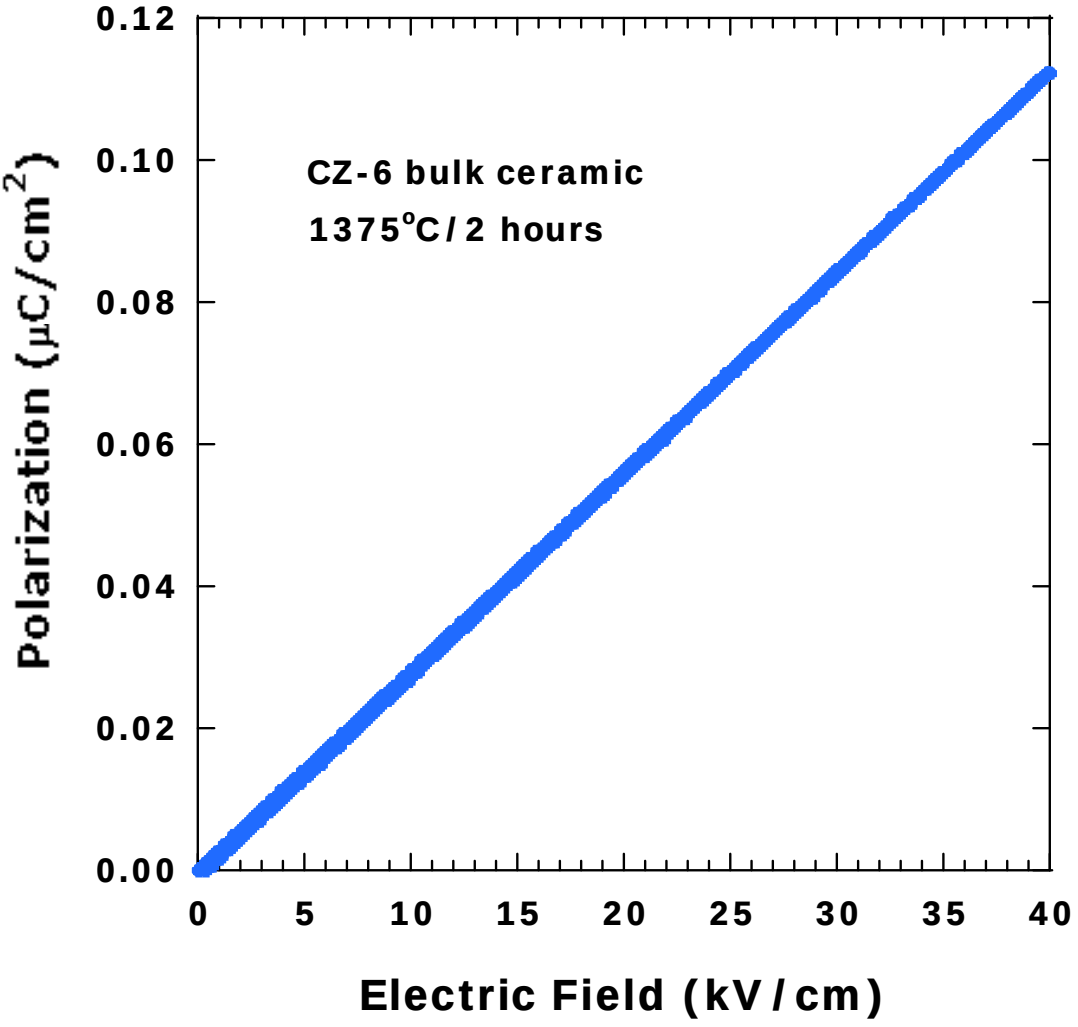

Figure 18. Polarization versus Field Characteristic for CZ–6 Ceramic fired at 1375°C/2 hours.

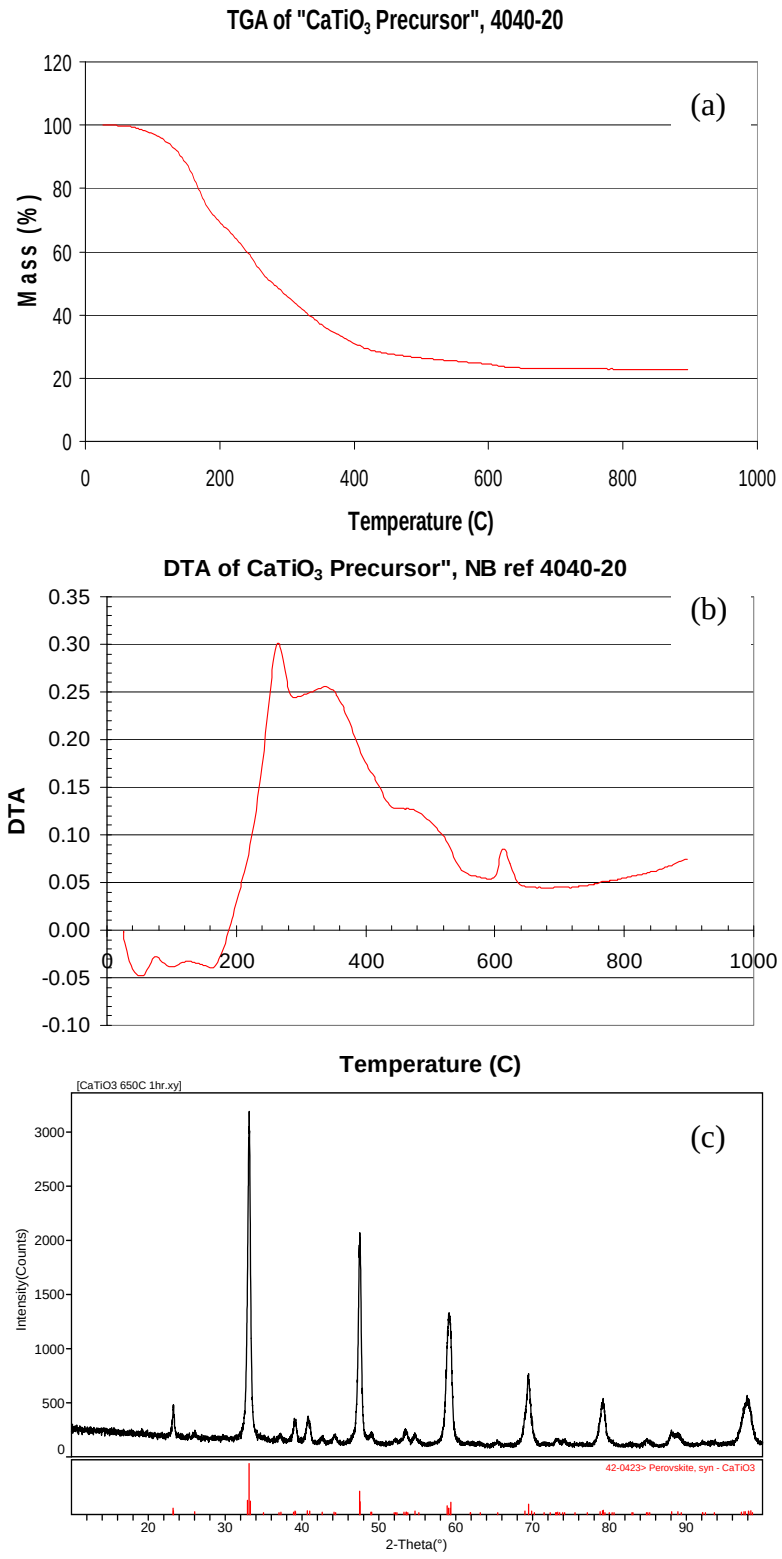

Figure 19. TGA (a) and DTA (b) of CT oxalate precursor. XRD (c) of calcined CT Ox at 640 °C, 1h to produce $CaTiO_3$.

3.6. Synthesis & Characterization of $CaTiO_3$ Powders

As previously mentioned, we have extended our synthetic route to include $CaTiO_3$ and results from the thermal analysis of CT Ox and XRD of the precursor calcined in air at 650 °C for 1h is shown in Figure 19. Here we used $Ti(OBu^n)_4$ in place of $Zr(OBu^n)_4$ and have continued to use $Ca(NO_3)_2$. An acac:Ti of 2:1 was also used during the synthesis. Thermal analysis on the resulting CT Ox undergoes solvent loss by ~ 200 °C and begins to decompose ~275 °C. Based on XRD of the calcined precursor, crystallization of $CaTiO_3$ begins at 600 °C. Through our non-aqueous synthesis, we were able to produce phase pure $CaTiO_3$ at 650 °C. In depth characterization of these powders are currently underway. We will use this synthetic route to produce $Ca(Zr_{1-X},Ti_X)O_3$ powders.

4. SUMMARY

$CaZrO_3$ and $CaTiO_3$ powders were synthesized using a non-aqueous oxalate co-precipitation route. Our goal was to prepare highly active powders that could be used to lower the sintering conditions (1500 °C) typically used for CT and CZ ceramics. Our route has been used to lower the sintering temperature for dense ceramics to 1375 °C and dielectric constants of ~30 have been achieved. These dielectric constants are comparable to those for conventional CZ dielectrics fired at the higher sintering temperature of 1500 ^{o}C. Several reaction, calcination, and sintering conditions were explored and the following recommendations have been made to aid in the development of larger scale quantities.

- Use acac:$M(OR)_x$ ratio of 2:1 to stabilize metals cation solution and provide phase pure CZ sintered pellets (1400° and 1375 °C) when powders are calcined at 650 °C, 54h for small scale reactions.
- A slurry age of 1h is sufficient.
- Shear mixing is necessary to produce a homogenous precipitate.
- Monitor oven drying conditions of CZ Ox precursor. Drying crystallizes CZ Ox and conditions used will change dehydration during decomposition.
- A fluorite $Ca_{0.5}Zr_{0.5}O_{1.5}$ phase is observed for stoichiometric Ca:Zr reactions at 650 °C, 1h. To convert to phase pure $CaZrO_3$ during sintering, use of powders calcined for long periods (10–54 h) is recommended for small scale. Large scale batches need further optimization.
- Accelerated shrinkage of pellets occurs at 1200 °C.
- Ball milling may be required to improve densification.

5. REFERENCES

1. Kell, R. C.; Riches, E. E.; Brigginshaw, P.; Olds, G. C. E.; Thomas, A. J.; Mayo, R. F.; Rendlf, D. F., *Electronics Letters* **1970,** 6, (19), 614-616.
2. Xu, J.; Wilkinson, A. P.; Pattanaik, S., *Chem. Mater.* **2000,** 12, 3321-3330.
3. Cavalcante, L. S.; Simoes, A. Z.; Espinosa, J. W. M.; Santos, L. P. S.; Longo, E.; Varela, J. A.; Pizani, P. S., *J Alloys and Compounds* **2008**, 340–346.
4. Reddy, V. B.; Mehrotra, P. N., *Z inorg, nucl. Chem.* **1981,** 3, 1078-1079.
5. Saavedra, M. J.; Parada, C.; Figueiredo, M. O.; Correa dos Santos, A., *Solid State Inonics* **1993,** 63-65, 213-217.
6. Rajendran, M.; Rao, M. S., *J. Mater. Res.* **1997,** 12, (10), 2665-2672.
7. Sekar, M. M. A.; Patil, K. C., *J. Mater. Chem.* **1992,** 2, 739-743.
8. Chapelet-Araba, B.; Nowogrockia, G.; Abrahama, F.; Grandjean, S., *J Solid State Chem.* **2004,** 177, 4269–4281.
9. Prasanth, C. S.; Kumar, H. P.; Pazhani, R.; Solomon, S.; Thomas, J. K., *Journal of Alloys and Compounds* **2008,** 464, 306–309.
10. Gonenli, I. E.; Tas, A. C., *J. Euro. Ceram. Soc.* **1999**, 2563-2567.
11. Pfaff, G., *Rec. Dev. Mater. Sci.* **2002,** 3, 59-67.
12. Li, Z.; Lee, W. E.; Zhang, S., *J. Am. Ceram. Soc.* **2007,** 90, (2), 364–368.
13. Pollet, M.; Marinel, S.; Roulland, F., *J. Euro. Ceram. Soc.* **2005,** 25, 2773–2777.
14. Ye, G.; Troczynski, T., *J. Am. Ceram. Soc.*, **2007,** 90, (1), 287–290.
15. Manik, S. K.; Pradhan, S. K., *J. Appl. Crystal.* **2005,** 38, 291–298.
16. Voigt, J. A.; Sipola, D. L.; Tuttle, B. A.; Anderson, M. T. Nonaqueous solution synthesis process for preparing oxide powders of lead zirconate titanate and related materials. US 5908802, 1990
17. Seidell, A., *Solubilities of Inorganic and Organic Compounds—A Compilation of Quantitative Solubility Data from the Periodical Literature*. D. Van Nostrand Co: 1919.
18. *Powder Diffraction file, ICDD, Newtown Square, PA.*
19. *PDF # 01-072-9960 Ca2:Zr (C2O4)4 (H2O)5* 2004.
20. *PDF #00-056-0178 + 01-074-4735 Ca2:Zr (C2O4)4 (H2O)5.5*, 2004 and 2005.
21. Gangadevi, T.; Muraleedharan, K.; Kannan, M. P., *Thermochimica Acta* **1989,** 146, 225-232.
22. Le, J.; van Rij, L. N.; van Landschoot, R. C.; Schoonman, J., *J. Euro. Ceram. Soc.* **1999,** 19, 2589±2591.
23. Krishnan, V.; Fergus, J. W., *J. Mater. Sci.* **2007,** 42, 6117–6122.
24. Lee, J.-S.; Park, J.-I.; Choi, T.-W., *J. Mater. Sci.* **1996,** 31, 2833-2838.
25. Kim, B.-H.; Lee, G.-Y.; Lee, W.-J.; Kim, J.-H., *Mater. Sci. Eng. B.* **2004,** 13, (3, 15), 198 - 202.
26. Shiozaki, Y.; Nokamura, E.; Mitsui, T.; Landolt-Bornstein, *Group III Condensed Matter* **1992,** Part of Subvolume A1 Oxides Vol. 36 Ferroelectrics and Related Substances, 10.1007/1042682_1042616.
27. Moulson, A. J.; Herbert, J. M., *Electroceramics Materials Properties Applications*. 2nd ed.; Chapman & Hall: London 1997.

DISTRIBUTION

4 Lawrence Livermore National Laboratory
Attn: N. Dunipace (1)
P.O. Box 808, MS L-795
Livermore, CA 94551-0808

1	MS1152	Kim Reed	1654
1	MS1152	Steve Glover	1654
11	MS0885	Justine Johannes	1810
	MS1349	William F. Hammetter	1815
1	MS1349	Bernadette A. Hernandez-Sanchez	1815
1	MS1411	James A Voigt	1816
1	MS1411	Bruce A. Tuttle	1816
1	MS1411	Diana Moore	1816
1	MS1411	Terry Garino	1816
1	MS1411	Patrick Mahoney	1816
1	MS1411	Mark A. Rodriguez	1822
1	MS0862	Barbara Wells	2732
1	MS0862	William Curtis III	2732
2	MS9018	Central Technical Files	8944
2	MS0899	Technical Library	4536


Sandia National Laboratories